1⁻⁻ and 0⁺⁺ heavy four-quark and molecule states in QCD

R.M. Albuquerque [a,b,1], F. Fanomezana [c,2], S. Narison [b,*], A. Rabemananjara [c,2]

[a] Instituto de Física, Universidade de São Paulo, C.P. 66318, 05389-970 São Paulo, SP, Brazil
[b] Laboratoire Particules et Univers de Montpellier, CNRS-IN2P3, Case 070, Place Eugène Bataillon, 34095 Montpellier, France
[c] Institute of High-Energy Physics of Madagascar (iHEP-MAD), University of Antananarivo, Madagascar

A R T I C L E   I N F O

A B S T R A C T

We estimate the masses of the 1^{--} heavy four-quark and molecule states by combining exponential Laplace (LSR) and finite energy (FESR) sum rules known perturbatively to lowest order (LO) in α_s but including non-perturbative terms up to the complete dimension-six condensate contributions. This approach allows to fix more precisely the value of the QCD continuum threshold (often taken ad hoc) at which the optimal result is extracted. We use double ratio of sum rules (DRSR) for determining the $SU(3)$ breakings terms. We also study the effects of the heavy quark mass definitions on these LO results. The $SU(3)$ mass-splittings of about (50–110) MeV and the ones of about (250–300) MeV between the lowest ground states and their 1st radial excitations are (almost) heavy-flavor independent. The mass predictions summarized in Table 4 are compared with the ones in the literature (when available) and with the three $Y_c(4260, 4360, 4660)$ and $Y_b(10\,890)$ 1^{--} experimental candidates. We conclude (to this order approximation) that the lowest observed state cannot be a *pure* 1^{--} four-quark nor a *pure* molecule but may result from their mixings. We extend the above analyzes to the 0^{++} four-quark and molecule states which are about (0.5–1) GeV heavier than the corresponding 1^{--} states, while the splittings between the 0^{++} lowest ground state and the 1st radial excitation is about (300–500) MeV. We complete the analysis by estimating the decay constants of the 1^{--} and 0^{++} four-quark states which are tiny and which exhibit a $1/M_Q$ behavior. Our predictions can be further tested using some alternative non-perturbative approaches or/and at LHC_b and some other hadron factories.

1. Introduction and a short review on the 1⁺⁺ channel

A large amount of exotic hadrons which differ from the "standard" $\bar{c}c$ charmonium and $\bar{b}b$ bottomium radial excitation states have been recently discovered in B-factories through $J/\psi\pi^+\pi^-$ and $\Upsilon\pi^+\pi^-$ processes and have stimulated different theoretical interpretations. Most of them have been assigned as four-quarks and/or molecule states [3]. In previous papers [1,2], some of us have studied, using exponential QCD spectral sum rules (QSSR) [4][3] and the double ratio of sum rules (DRSR) [7],[4] the nature of the $X(3872)$ 1^{++} states found by Belle [11] and confirmed by

BaBar [12], CDF [13] and D0 [14]. If it is a $(cq)(\bar{c}\bar{q})$ four-quark or D–D^* molecule state, one finds for $m_c = 1.23$ GeV [1][5]:

$$X_c = (3925 \pm 127)\ \text{MeV}, \tag{1}$$

corresponding to a t_c-value common solution of the exponential Laplace (LSR) and Finite Energy (FESR) sum rules:

$$\sqrt{t_c} = (4.15 \pm 0.03)\ \text{GeV}, \tag{2}$$

while in the b-meson channel, using $m_b = 4.26$ GeV, one finds [1]:

$$X_b = (10\,144 \pm 104)\ \text{MeV} \quad \text{with} \quad \sqrt{t_c} = (10.4 \pm 0.02)\ \text{GeV}, \tag{3}$$

where a similar result has been found in [15] using another choice of interpolating current. However, in the case of the $X_c(3872)$, the previous two configurations are not favored by its narrow hadronic width ($\leqslant 2.3$ MeV), which has lead some of us to propose that it could be, instead, a λ–J/ψ-type molecule [2] described by the current:

---

* Corresponding author.
  E-mail addresses: rma@if.usp.br (R.M. Albuquerque), fanfenos@yahoo.fr
(F. Fanomezana), snarison@yahoo.fr (S. Narison), achris_01@yahoo.fr
(A. Rabemananjara).

[1] FAPESP CNPq-Brasil PhD student fellow.
[2] PhD student.
[3] For reviews, see e.g. [5,6].
[4] For some other successful applications, see [8–10].

[5] The two configurations give almost a degenerate mass-value [2].

$$J_\mu^\lambda = \left(\frac{g}{\Lambda}\right)^2_{\text{eff}} (\bar{c}\lambda^a \gamma^\mu c)(\bar{q}\lambda_a \gamma_5 q), \tag{4}$$

where λ_a is the color matrix, while g and Λ are coupling and scale associated to an effective Van der Vaals force. In this case, the narrow width of the X_c is mainly due to the extra-gluon exchange which gives a suppression of the order α_s^2 compared to the two former configurations, if one evaluates this width using vertex sum rules. The corresponding mass is slightly lower than the one in Eq. (1) [2]:

$$r \equiv \frac{X_c^\lambda}{X_c^{mol}} = 0.96 \pm 0.03 \quad \Longrightarrow \quad X_c^\lambda = (3768 \pm 127)\ \text{MeV}, \tag{5}$$

which (within the errors) also agree with the data. By assuming that the mass of the radial excitation $X_Q' \approx \sqrt{t_c}$, one can also deduce the mass-splitting:

$$X_c' - X_c \simeq 225\ \text{MeV} \approx X_b' - X_b \simeq 256\ \text{MeV}, \tag{6}$$

which is much lower than the ones of ordinary charmonium and bottomium states:

$$\psi(2S) - \psi(1S) \simeq 590 \approx \Upsilon(2S) - \Upsilon(1S) \simeq 560\ \text{MeV}, \tag{7}$$

and suggests a completely different dynamics for these exotic states. Comparing the previous results with the observed $Z_b(10\,610)$ and $Z_b(10\,650)$ states by Belle [16] whose quantum numbers have been assigned to be 1^{++}, one can conclude that these observed states are heavier than the 1st radial excitation of the $X_b(10.14)$ expected from QSSR to lowest order in α_s [1].

2. QCD Analysis of the 1^{--} and 0^{++} channels

In the following, we extend the previous analysis to the case of the 1^{--} and 0^{++} channels and improve some existing analysis from QCD (spectral) sum rules in the 1^{--} channel [17]. The results will be compared with the experimental 1^{--} candidate states:

$$Y_c(4260), \quad Y_c(4360), \quad Y_c(4660), \quad Y_b(10\,890). \tag{8}$$

The Y_c have been seen by CLEO [18], BaBar [19], Belle [20] and CDF [21], in the decay into $J/\psi\pi^+\pi^-$ while Y_b is seen from $\Upsilon\pi^+\pi^-$ by Belle [22] around the $\Upsilon(5S)$ mass. These states cannot be identified with standard $\bar{c}c$ charmonium and $\bar{b}b$ bottomium radial excitations and have been assigned in the literature to be four-quark or molecule states or some threshold effects.

2.1. QCD input parameters

The QCD parameters which shall appear in the following analysis will be the charm and bottom quark masses $m_{c,b}$, the light quark masses $m_{d,s}$, the light quark condensates $\langle \bar{q}q \rangle$ and $\langle \bar{s}s \rangle$, the gluon condensates $\langle g^2 G^2 \rangle \equiv \langle g^2 G_{\mu\nu}^a G_a^{\mu\nu} \rangle$ and $\langle g^3 G^3 \rangle \equiv \langle g^3 f_{abc} G_{\mu\nu}^a G_{\nu\rho}^b G_{\rho\mu}^c \rangle$, the mixed condensate $\langle \bar{q}g\sigma Gq \rangle \equiv \langle \bar{q}g\sigma^{\mu\nu} (\lambda_a/2)G_{\mu\nu}^a q \rangle$ and the four-quark condensate $\rho\langle \bar{q}q \rangle^2$, where ρ indicates the violation of the four-quark vacuum saturation. Their values are given in Table 1 and we shall work with the running light quark parameters:

$$\bar{m}_s(\tau) = \frac{\hat{m}_s}{(-\log\sqrt{\tau}\Lambda)^{-2/\beta_1}},$$

$$\langle \bar{q}q \rangle(\tau) = -\hat{\mu}_q^3(-\log\sqrt{\tau}\Lambda)^{-2/\beta_1},$$

$$\langle \bar{q}g\sigma Gq \rangle(\tau) = -M_0^2\hat{\mu}_q^3(-\log\sqrt{\tau}\Lambda)^{-1/3\beta_1}, \tag{9}$$

where $\beta_1 = -(1/2)(11 - 2n/3)$ is the first coefficient of the β function for n flavors; $\hat{m}_s$ and $\hat{\mu}_q$ are renormalization group invariant light quark mass and condensate [24,25].

Table 1
QCD input parameters. For the heavy quark masses, we use the range spanned by the running $\overline{\text{MS}}$ mass $\bar{m}_Q(M_Q)$ and the on-shell mass from QCD (spectral) sum rules compiled in pages 602 and 603 of the book in [5] and recently obtained in Ref. [27]. The values of Λ and $\hat{\mu}_q$ have been obtained from $\alpha_s(M_\tau) = 0.325(8)$ [28] and from the running masses: $(\bar{m}_u + \bar{m}_d)(2) = 7.9(3)$ MeV [30]. The original errors have been multiplied by 2 for a conservative estimate of the errors.

Parameters	Values	Refs.
$\Lambda(n_f = 4)$	(324 ± 15) MeV	[28,29,31]
$\Lambda(n_f = 5)$	(194 ± 10) MeV	[28,29,31]
$\hat{m}_s$	(0.114 ± 0.021) GeV	[5,30,31]
m_c	$(1.26–1.47)$ GeV	[5,27,30–33]
m_b	$(4.17–4.70)$ GeV	[5,27,30–32]
$\hat{\mu}_q$	(263 ± 7) MeV	[5,30]
$\kappa \equiv \langle \bar{s}s \rangle / \langle \bar{u}u \rangle$	(0.74 ± 0.06)	[9]
M_0^2	(0.8 ± 0.2) GeV^2	[34–36]
$\langle \alpha_s G^2 \rangle$	$(7 \pm 2) \times 10^{-2}$ GeV^4	[27,28,37–43]
$\langle g^3 G^3 \rangle$	(8.3 ± 1.0) GeV$^2 \times \langle \alpha_s G^2 \rangle$	[27]
$\rho \equiv \langle \bar{q}q\bar{q}q \rangle / \langle \bar{q}q \rangle^2$	(2 ± 1)	[28,34,37]

2.2. Interpolating currents

We assume that the Y state is described either by the lowest dimension (without derivative terms) four-quark and molecule $\bar{D}_s D_s^*$ vector currents J_μ given in Tables 2 and 3. Unlike the case of baryons where both positive and parity states can couple to the same operator [23], the situation is simpler here as the vector and axial-vector currents have a well-defined quantum numbers to which are associated the 1^{--} (resp. 1^{++}) states for the transverse part and the 0^{++} (resp. 0^{--}) states for the longitudinal part. In the case of four-quark currents, we can have two-types of lowest derivative vector operators which can mix through the mixing parameter b.[6] Another possible mixing can occur through the renormalization of operators [25,26] though this type of mixing will only induce an overall effect due to the anomalous dimension which will be relevant at higher order in α_s but will disappear in the ratio of sum rules used in this Letter. For the molecule current, we choose the product of local bilinear current which has the quantum number of the corresponding meson state. In this sense, we have only an unique interpolating current. Observed states can be a mixing of different states associated to each choice of operators and their selection can only be done through the analysis of their decays [2] but this is beyond the scope of this Letter.

2.3. The two-point function in QCD

The two-point functions of the Y_Q ($Q \equiv c, b$) (assumed to be a 1^{--} vector meson) is defined as:

$$\Pi^{\mu\nu}(q) \equiv i \int d^4x\, e^{iq\cdot x} \langle 0|T[j^\mu(x)j^{\nu\dagger}(0)]|0 \rangle$$

$$= -\Pi^{(1)}(q^2)\left(g^{\mu\nu} - \frac{q_\mu q_\nu}{q^2}\right) + \Pi^{(0)}(q^2)\frac{q^\mu q^\nu}{q^2}, \tag{10}$$

where J^μ are the interpolating vector currents given Tables 2 and 3. We assume that the Y state is described either by the lowest dimension (without derivative terms) four-quark and molecule $\bar{D}_s D_s^*$ currents given in Tables 2 and 3. The two invariants, $\Pi^{(1)}$ and $\Pi^{(0)}$, appearing in Eq. (10) are independent and have respectively the quantum numbers of the spin 1 and 0 mesons. We can extract $\Pi_Q^{(1)}$ and $\Pi^{(0)}(q^2)$ or the corresponding spectral functions from the complete expression of $\Pi_Q^{\mu\nu}(q)$ by applying respectively to it the projectors:

---

[6] The 1^{++} four-quark state described by the axial-vector current has been analyzed in [1,2].

Table 2

QCD expression of the four-quark spectral functions to lowest order in α_s and up to dimension-six condensates: $Q \equiv c, b$ is the heavy quark field.

Current	$j_{4q}^{\mu} = \frac{\epsilon_{abc}\epsilon_{dec}}{\sqrt{2}} \{[(s_a^T C\gamma_5 Q_b)(\bar{s}_d\gamma^\mu\gamma_5 C\bar{Q}_e^T) + (s_a^T C\gamma_5\gamma^\mu Q_b)(\bar{s}_d\gamma_5 C\bar{Q}_e^T)] + b[(s_a^T C Q_b)(\bar{s}_d\gamma^\mu C\bar{Q}_e^T) + (s_a^T C\gamma^\mu Q_b)(\bar{s}_d C\bar{Q}_e^T)]\}$
1^{--}	Spectral function $\frac{1}{\pi}\operatorname{Im}\Pi^{(1)}(s)$
Pert	$-\frac{1}{3 \cdot 2^{10}\pi^6}\int_{\alpha_{min}}^{\alpha_{max}}\frac{d\alpha}{\alpha^3}\int_{\beta_{min}}^{1-\alpha}\frac{d\beta}{\beta^3}(1-\alpha-\beta)[2m_Q^2(1-b^2)(1-\alpha-\beta)^2\mathcal{F}_3 - 3(1+b^2)(1+\alpha+\beta)\mathcal{F}_4 + 12b^2 m_Q m_s(1-\alpha-\beta)(\alpha+\beta)\mathcal{F}_3]$,
$\langle\bar{s}s\rangle$	$\frac{\langle\bar{s}s\rangle}{2^5\pi^4}\int_{\alpha_{min}}^{\alpha_{max}}\frac{d\alpha}{\alpha^2}\{\frac{m_s(1+b^2)\alpha}{(1-\alpha)}\mathcal{H}_2 - \int_{\beta_{min}}^{1-\alpha}\frac{d\beta}{\beta^2}[b^2 m_Q(1-\alpha-\beta)(\alpha+\beta)\mathcal{F}_2 + m_s\alpha\beta(m_Q^2(5-\alpha-\beta+b^2(3+\alpha+\beta))\mathcal{F}_1 + 2\mathcal{F}_2)]\}$,
$\langle G^2\rangle$	$-\frac{\langle g^2 G^2\rangle}{3^2 \cdot 2^{11}\pi^6}\int_{\alpha_{min}}^{\alpha_{max}}\frac{d\alpha}{\alpha}\int_{\beta_{min}}^{1-\alpha}\frac{d\beta}{\beta^3}\{2m_Q^4(1-b^2)\alpha(1-\alpha-\beta)^3 - 3m_Q^2(1-\alpha-\beta)[8\alpha(1+\alpha+\beta) - (1-b^2)(2-\beta+(6\alpha-\beta)(\alpha+\beta))]\mathcal{F}_1$
	$\quad + 6(1+b^2)\beta(1-2\alpha-2\beta)\mathcal{F}_2\}$,
$\langle\bar{s}Gs\rangle$	$\frac{\langle\bar{s}Gs\rangle}{3 \cdot 2^7\pi^4}\{3m_Q\int_{\alpha_{min}}^{\alpha_{max}}\frac{d\alpha}{\alpha}\int_{\beta_{min}}^{1-\alpha}\frac{d\beta}{\beta^2}[2\beta(1-2\alpha-2\beta) + (1-b^2)(2\alpha(\alpha+\beta) - \beta(1-3\alpha-3\beta))]\mathcal{F}_1$
	$\quad - m_s\int_{\alpha_{min}}^{\alpha_{max}}d\alpha[\frac{2}{\alpha}(8m_Q^2\alpha(1+b^2) + (1-\alpha+b^2(1-7\alpha))\mathcal{H}_1) + \int_{\beta_{min}}^{1-\alpha}\frac{d\beta}{\beta}(m_Q^2(6+3\alpha-5\beta+b^2(6-3\alpha+5\beta)) + 3(7+b^2)\mathcal{F}_1)]\}$,
$\langle\bar{s}s\rangle^2$	$-\frac{\rho\langle\bar{s}s\rangle^2}{3 \cdot 2^3\pi^2}\int_{\alpha_{min}}^{\alpha_{max}}d\alpha[4m_Q^2 - (1-b^2)(2m_Q^2 - \mathcal{H}_1) + m_s m_Q b^2]$,
$\langle G^3\rangle$	$\frac{\langle g^3 G^3\rangle}{3^3 \cdot 2^{11}\pi^6}\{3\int_{\alpha_{min}}^{\alpha_{max}}\frac{d\alpha}{\alpha}\int_{\beta_{min}}^{1-\alpha}\frac{d\beta}{\beta^3}(1-\alpha-\beta)[m_Q^2(12\alpha^2(1+\alpha+\beta) - (1-b^2)(3\alpha(1+3\alpha^2+3\beta^2) + 2\beta(14+4\alpha+11\alpha^2 - (1+\alpha)(9+4\alpha+9\beta))))$
	$\quad + 3\alpha(1+b^2)(1+\alpha+\beta)\mathcal{F}_1] + m_Q^4(1-b^2)\int_0^1\frac{d\alpha}{\alpha}\int_0^1\frac{d\beta}{\beta^4}(1-\alpha-\beta)^2(3\alpha+4\beta)\delta(s - \frac{(\alpha+\beta)}{\alpha\beta}m_Q^2)\}$.
0^{++}	Spectral function $\frac{1}{\pi}\operatorname{Im}\Pi^{(0)}(s)$
Pert	$-\frac{1}{3 \cdot 2^{10}\pi^6}\int_{\alpha_{min}}^{\alpha_{max}}\frac{d\alpha}{\alpha^3}\int_{\beta_{min}}^{1-\alpha}\frac{d\beta}{\beta^3}(1-\alpha-\beta)[12m_Q^4(1-b^2)(\alpha+\beta)(1-\alpha-\beta)^2\mathcal{F}_2 - 2m_Q^2(1-\alpha-\beta)(7-19\alpha-19\beta-b^2(7+5\alpha+5\beta))\mathcal{F}_3$
	$\quad - 3(1+b^2)(7-9\alpha-9\beta)\mathcal{F}_4 + 12b^2 m_Q m_s(1-\alpha-\beta)^2(\alpha+\beta)(6m_Q^2(\alpha+\beta)\mathcal{F}_2 - 7\mathcal{F}_3)]$,
$\langle\bar{s}s\rangle$	$-\frac{\langle\bar{s}s\rangle}{2^5\pi^4}\int_{\alpha_{min}}^{\alpha_{max}}\frac{d\alpha}{\alpha^2}\{\frac{m_s(1+b^2)\alpha}{(1-\alpha)}\mathcal{H}_2 + \int_{\beta_{min}}^{1-\alpha}\frac{d\beta}{\beta^2}[b^2 m_Q(1-\alpha-\beta)(\alpha+\beta)(4m_Q^2(\alpha+\beta)\mathcal{F}_1 - 5\mathcal{F}_2)$
	$\quad + m_s\alpha\beta(2m_Q^4(1-b^2)(1-\alpha-\beta)(\alpha+\beta) - m_Q^2(7-11\alpha-11\beta+b^2(1+3\alpha+3\beta))\mathcal{F}_1 - 10\mathcal{F}_2)]\}$,
$\langle G^2\rangle$	$-\frac{\langle g^2 G^2\rangle}{3^2 \cdot 2^{11}\pi^6}\{\int_{\alpha_{min}}^{\alpha_{max}}\frac{d\alpha}{\alpha}\int_{\beta_{min}}^{1-\alpha}\frac{d\beta}{\beta^3}[2m_Q^4(1-\alpha-\beta)^2(24\alpha(\alpha+\beta) + (1-b^2)(\alpha(5-17\alpha-17\beta) + 3\beta(2+\alpha+\beta)))$
	$\quad - 3m_Q^2(1-\alpha-\beta)(8\alpha(1-3\alpha-3\beta) - 32\beta(\alpha+\beta) + (1-b^2)(6-2\alpha(8-9\alpha-9\beta) - \beta(3-13\alpha-13\beta)))\mathcal{F}_1 - 6(1+b^2)\beta(9-10\alpha-10\beta)\mathcal{F}_2]$
	$\quad - 4m_Q^6(1-b^2)\int_0^1\frac{d\alpha}{\alpha}\int_0^1\frac{d\beta}{\beta^4}(\alpha+\beta)(1-\alpha-\beta)^3\delta(s - \frac{(\alpha+\beta)}{\alpha\beta}m_Q^2)\}$,
$\langle\bar{s}Gs\rangle$	$\frac{\langle\bar{s}Gs\rangle}{3 \cdot 2^7\pi^4}\{3m_Q\int_{\alpha_{min}}^{\alpha_{max}}\frac{d\alpha}{\alpha}\int_{\beta_{min}}^{1-\alpha}\frac{d\beta}{\beta^2}[(2m_Q^2(\alpha+\beta) - 3\mathcal{F}_1)(2\beta(1-2\alpha-2\beta) - (1-b^2)(2\alpha(1-\alpha-\beta) + \beta(1-3\alpha-3\beta))) - 2\alpha(1-b^2)\mathcal{F}_1]$
	$\quad - m_s\int_{\alpha_{min}}^{\alpha_{max}}d\alpha[\frac{2}{\alpha}(2m_Q^2\alpha(1-5b^2) - (2-(1-b^2)(1-9\alpha))\mathcal{H}_1) + \int_{\beta_{min}}^{1-\alpha}\frac{d\beta}{\beta}(m_Q^2(4(3-4\alpha-4\beta) - (1-b^2)(3+\alpha+3\beta)) + 3(7+b^2)\mathcal{F}_1)]$
	$\quad - 2m_s m_Q^4(1-b^2)\int_0^1\frac{d\alpha}{\alpha}\int_0^1\frac{d\beta}{\beta^2}(3-3\alpha-5\beta)(\alpha+\beta)\delta(s - \frac{(\alpha+\beta)}{\alpha\beta}m_Q^2)\}$,
$\langle\bar{s}s\rangle^2$	$\frac{\rho\langle\bar{s}s\rangle^2}{3 \cdot 2^3\pi^2}\{\int_{\alpha_{min}}^{\alpha_{max}}d\alpha[4m_Q^2 - (1-b^2)(4m_Q^2 - 3\mathcal{H}_1) + m_s m_Q b^2] + 2m_s m_Q^3 b^2\int_0^1\frac{d\alpha}{\alpha(1-\alpha)}\delta(s - \frac{m_Q^2}{\alpha(1-\alpha)})\}$,
$\langle G^3\rangle$	$-\frac{\langle g^3 G^3\rangle}{3^3 \cdot 2^{11}\pi^6}\{3\int_{\alpha_{min}}^{\alpha_{max}}\frac{d\alpha}{\alpha^2}\int_{\beta_{min}}^{1-\alpha}\frac{d\beta}{\beta^3}(1-\alpha-\beta)[m_Q^2(12\alpha^2(\alpha(2-\beta) + \beta(1-\beta)) - (1-b^2)(3\alpha^2(1+\alpha)^2 + \beta^2(10-\alpha(5\alpha+8) - 2\beta(6-\beta))))$
	$\quad - 3\alpha^2(1+b^2)(1-3\alpha-3\beta)\mathcal{F}_1] + m_Q^4\int_0^1\frac{d\alpha}{\alpha^2}\int_0^1\frac{d\beta}{\beta^5}(1-\alpha-\beta)^2\delta(s - \frac{(\alpha+\beta)}{\alpha\beta}m_Q^2)[72\alpha^2\beta(\alpha+\beta)$
	$\quad + (1-b^2)\beta(3(7-19\alpha)\alpha^2 + 2(6-5\alpha)\beta^2 + (34-91\alpha)\alpha\beta) - 2m_Q^2\tau(1-b^2)(1-\alpha-\beta)(\alpha+\beta)(3\alpha+4\beta)]\}$.
with:	$\mathcal{F}_k = [m_Q^2(\alpha+\beta) - \alpha\beta s]^k, \qquad \mathcal{H}_k = [m_Q^2 - \alpha(1-\alpha)s]^k, \qquad \beta_{min} = \alpha m_Q^2/(s\alpha - m_Q^2),$
	$\alpha_{min} = \frac{1}{2}(1-v), \qquad \alpha_{max} = \frac{1}{2}(1+v), \qquad v \text{ the } Q\text{-quark velocity: } v \equiv \sqrt{1 - 4m_Q^2/s} \text{ and } z \equiv \frac{m_Q^2(\alpha+\beta)}{\alpha\beta}.$

$$\mathcal{P}_{\mu\nu}^{(1)} = -\frac{1}{3}\left(g^{\mu\nu} - \frac{q^\mu q^\nu}{q^2}\right) \quad \text{and} \quad \mathcal{P}_{\mu\nu}^{(0)} = \frac{q_\mu q_\nu}{q^2}. \tag{11}$$

Due to its analyticity, the correlation function, $\Pi^{(1,0)}(q^2)$ in Eq. (10), obeys the dispersion relation:

$$\Pi^{(1,0)}(q^2) = \frac{1}{\pi}\int_{4m_c^2}^{\infty} ds\, \frac{\operatorname{Im}\Pi^{(1,0)}(s)}{s - q^2 - i\epsilon} + \cdots, \tag{12}$$

where $\operatorname{Im}\Pi^{(1,0)}(s)$ are the spectral functions. The QCD expressions of these spectral functions are given in Tables 2 and 3. $1/q^2$ terms discussed in [44,45], which are dual to higher order terms of the QCD series will not be included here as we work to leading order.

3. 1^{--} four-quark state mass Y_{Qq} from QSSR

In the following, we shall estimate the mass of the 1^{--} four-quark state $(\overline{Qq})(Qq)$ ($Q \equiv c, b$ and $q \equiv u, d$ quarks), hereafter denoted by Y_{Qd}. In so doing, we shall use the ratios of the Laplace (exponential) sum rule:

$$\mathcal{R}_{Qd}^{LSR}(\tau) \equiv -\frac{d}{d\tau}\log\int_{t_<}^{t_c} dt\, e^{-t\tau}\frac{1}{\pi}\operatorname{Im}\Pi^{(1)}(t), \tag{13}$$

and of FESR:

$$\mathcal{R}_{Qd}^{FESR} \equiv \frac{\int_{t_<}^{t_c} dt\, t^n\frac{1}{\pi}\operatorname{Im}\Pi^{(1)}(t)}{\int_{t_<}^{t_c} dt\, t^{n-1}\frac{1}{\pi}\operatorname{Im}\Pi^{(1)}(t)}: \quad n = 1, \tag{14}$$

where $t_<$ is the hadronic (quark) threshold. Within the usual duality ansatz "one resonance" $+ \theta(t - t_c) \times QCD$ continuum parametrization of the spectral function, the previous ratios of sum rules give:

$$\mathcal{R}_{Qd}^{LSR}(\tau) \simeq M_{Y_{Qd}}^2 \simeq \mathcal{R}_{Qd}^{FESR}. \tag{15}$$

For a discussion more closed to the existing literature which we shall test the reliability in the following, we start to work with the current corresponding to $b = 0$. We shall discuss the more general choice of current when b is a free parameter at the end of this section.

3.1. The Y_{cd} mass from LSR and FESR for the case $b = 0$

Using the QCD inputs in Table 1, we show the τ-behavior of $M_{Y_{cd}}$ from $\mathcal{R}_{cd}^{LSR}$ in Fig. 1(a) for $m_c = 1.26$ GeV and for different values of t_c. One can notice from Fig. 1(a) that the τ-stability is obtained from $\sqrt{t_c} \geqslant 5.1$ GeV, while the t_c-stability is reached for $\sqrt{t_c} = 7$ GeV. The most conservative prediction from the LSR is

Table 3

QCD expression of the molecule spectral functions to lowest order in α_s and up to dimension-six condensates: $Q \equiv c, b$ is the heavy quark field, while g' and Λ' are coupling and scale associated to an effective Van Der Vaals force.

Current	$j_{mol}^{\mu} = \frac{1}{\sqrt{2}}\left(\frac{g'}{\Lambda'^2}\right)^2_{eff}[(\bar{s}\gamma^{\mu}Q)(\bar{Q}s) + (\bar{Q}\gamma^{\mu}s)(\bar{s}Q)]$
1^{--}	Spectral function $\frac{1}{\pi}\operatorname{Im}\Pi^{(1)}(s)$
Pert	$-\frac{1}{2^{12}\pi^6}\int_{\alpha_{min}}^{\alpha_{max}}\frac{d\alpha}{\alpha^3}\int_{\beta_{min}}^{1-\alpha}\frac{d\beta}{\beta^3}(1-\alpha-\beta)\mathcal{F}_3[2m_Q^2(1-\alpha-\beta)^2 - 3(1+\alpha+\beta)\mathcal{F}_1]$,
$\langle \bar{s}s \rangle$	$\frac{3m_s\langle\bar{s}s\rangle}{2^7\pi^4}\left\{\int_{\alpha_{min}}^{\alpha_{max}}\frac{d\alpha}{\alpha(1-\alpha)}\mathcal{H}_2 - \int_{\alpha_{min}}^{\alpha_{max}}\frac{d\alpha}{\alpha}\int_{\beta_{min}}^{1-\alpha}\frac{d\beta}{\beta}\mathcal{F}_1[m_Q^2(5-\alpha-\beta)+2\mathcal{F}_1]\right\}$,
$\langle G^2 \rangle$	$-\frac{\langle g^2 G^2\rangle}{3\cdot2^{12}\pi^6}\int_{\alpha_{min}}^{\alpha_{max}}\frac{d\alpha}{\alpha}\int_{\beta_{min}}^{1-\alpha}\frac{d\beta}{\beta^3}\{m_Q^4\alpha(1-\alpha-\beta)^3 + 3m_Q^2(1-\alpha-\beta)[1-\alpha(4+\alpha+\beta)+\beta(1-2\alpha-2\beta)]\mathcal{F}_1 + 6\beta(1-2\alpha-2\beta)\mathcal{F}_2\}$,
$\langle \bar{s}Gs \rangle$	$\frac{\langle\bar{s}gGs\rangle}{2^8\pi^4}\{3m_Q\int_{\alpha_{min}}^{\alpha_{max}}\frac{d\alpha}{\alpha^2}\int_{\beta_{min}}^{1-\alpha}\frac{d\beta}{\beta}(\alpha^2-\alpha(1+\beta)-2\beta^2)\mathcal{F}_1 - m_s[\int_{\alpha_{min}}^{\alpha_{max}}\frac{d\alpha}{\alpha}(8m_Q^2\alpha+(2-\alpha)\mathcal{H}_1) - \int_{\alpha_{min}}^{\alpha_{max}}d\alpha\int_{\beta_{min}}^{1-\alpha}\frac{d\beta}{\beta}(m_Q^2(9-3\alpha-4\beta)+7\mathcal{F}_1)]\}$,
$\langle \bar{s}s \rangle^2$	$-\frac{\rho\langle\bar{s}s\rangle^2}{2^6\pi^2}\int_{\alpha_{min}}^{\alpha_{max}}d\alpha[3m_Q^2-\alpha(1-\alpha)s]$,
$\langle G^3 \rangle$	$-\frac{\langle g^3 G^3\rangle}{5\cdot3\cdot2^{16}\pi^6}\{5\int_{\alpha_{min}}^{\alpha_{max}}d\alpha\int_{\beta_{min}}^{1-\alpha}\frac{d\beta}{\beta^3}(1-\alpha-\beta)[m_Q^2(5\alpha^2-\alpha(37-19\beta)+14(1-\beta)^2)-3(7+9\alpha+9\beta)\mathcal{F}_1]$
	$\quad + m_Q^4\int_0^1 d\alpha\int_0^1\frac{d\beta}{\beta^5}e^{-\frac{(\alpha+\beta)}{\alpha\beta}m_Q^2\tau}(1-\alpha-\beta)[2m_Q^2\tau(1-\alpha-\beta)^2-\beta(50\alpha^2-\alpha(61-85\beta)+35(1-\beta)^2)]\}$.
0^{++}	Spectral function $\frac{1}{\pi}\operatorname{Im}\Pi^{(0)}(s)$
Pert	$-\frac{1}{2^{12}\pi^6}\int_{\alpha_{min}}^{\alpha_{max}}\frac{d\alpha}{\alpha^3}\int_{\beta_{min}}^{1-\alpha}\frac{d\beta}{\beta^3}(1-\alpha-\beta)[12m_Q^4(\alpha+\beta)(1-\alpha-\beta)^2\mathcal{F}_2 - 2m_Q^2(1-\alpha-\beta)(7-19\alpha-19\beta)\mathcal{F}_3 - 3(7-9\alpha-9\beta)\mathcal{F}_4]$,
$\langle \bar{s}s \rangle$	$-\frac{3m_s\langle\bar{s}s\rangle}{2^7\pi^4}\{\int_{\alpha_{min}}^{\alpha_{max}}d\alpha\frac{\mathcal{H}_2}{\alpha(1-\alpha)} + \int_{\alpha_{min}}^{\alpha_{max}}\frac{d\alpha}{\alpha}\int_{\beta_{min}}^{1-\alpha}\frac{d\beta}{\beta}[2m_Q^4(\alpha+\beta)(1-\alpha-\beta)-m_Q^2(7-11\alpha-11\beta)\mathcal{F}_1-10\mathcal{F}_2]\}$,
$\langle G^2 \rangle$	$-\frac{\langle g^2 G^2\rangle}{3\cdot2^{12}\pi^6}\{\int_{\alpha_{min}}^{\alpha_{max}}\frac{d\alpha}{\alpha}\int_{\beta_{min}}^{1-\alpha}\frac{d\beta}{\beta^3}[m_Q^4(1-\alpha-\beta)^2(7\alpha^2+\alpha(5+19\beta)+6\beta(1+2\beta))$
	$\quad + 3m_Q^2(1-\alpha-\beta)(3\alpha^2+\alpha(4+25\beta)-\beta(3-22\beta)-3)\mathcal{F}_1 - 6\beta(9-10\alpha-10\beta)\mathcal{F}_2] - 2m_Q^6\int_0^1 d\alpha\int_0^1 d\beta\frac{(\alpha+\beta)(1-\alpha-\beta)^3}{\alpha\beta^4}e^{-\frac{(\alpha+\beta)}{\alpha\beta}m_Q^2\tau}\}$,
$\langle \bar{s}Gs \rangle$	$-\frac{\langle\bar{s}gGs\rangle}{2^8\pi^4}\{3m_Q\int_{\alpha_{min}}^{\alpha_{max}}\frac{d\alpha}{\alpha^2}\int_{\beta_{min}}^{1-\alpha}\frac{d\beta}{\beta}[2m_Q^2(1-\alpha-\beta)(\alpha+\beta)(\alpha-2\beta)+(3\alpha^2-3\alpha(1+\beta)+2\beta(2-3\beta))\mathcal{F}_1]$
	$\quad + m_s\int_{\alpha_{min}}^{\alpha_{max}}\frac{d\alpha}{\alpha}[2m_Q^2\alpha-(2+9\alpha)\mathcal{H}_1] + m_s\int_{\alpha_{min}}^{\alpha_{max}}d\alpha\int_{\beta_{min}}^{1-\alpha}\frac{d\beta}{\beta}(m_Q^2(9-17\alpha-18\beta)+21\mathcal{F}_1) + 2m_sm_Q^4\int_0^1 d\alpha\int_0^1 d\beta\frac{(\alpha+\beta)(3-3\alpha-4\beta)}{\alpha\beta^2}e^{-\frac{(\alpha+\beta)}{\alpha\beta}m_Q^2\tau}\}$,
$\langle \bar{s}s \rangle^2$	$\frac{3\rho\langle\bar{s}s\rangle^2}{2^5\pi^2}\int_{\alpha_{min}}^{\alpha_{max}}d\alpha[m_Q^2-\alpha(1-\alpha)s]$,
$\langle G^3 \rangle$	$\frac{\langle g^3 G^3\rangle}{5\cdot3\cdot2^{16}\pi^6}\{5\int_{\alpha_{min}}^{\alpha_{max}}d\alpha\int_{\beta_{min}}^{1-\alpha}\frac{d\beta}{\beta^3}(1-\alpha-\beta)[m_Q^2(59\alpha^2-\alpha(91-127\beta)+14-2\beta(41-34\beta))+(33-81\alpha-81\beta)\mathcal{F}_1]$
	$\quad + m_Q^4\int_0^1\frac{d\alpha}{\alpha}\int_0^1\frac{d\beta}{\beta^6}(1-\alpha-\beta)e^{-\frac{(\alpha+\beta)}{\alpha\beta}m_Q^2\tau}[4m_Q^4\tau^2(\alpha+\beta)(1-\alpha-\beta)^2+2m_Q^2\tau\beta(1-\alpha-\beta)(53\alpha^2-\alpha(38-88\beta)-35\beta(1-\beta))$
	$\quad + \beta^2(100\alpha^3+140\beta(1-\beta)^2-13\alpha^2(23-25\beta)+5\alpha(1-\beta)(35-73\beta))]\}$.

obtained in this range of t_c-values for $m_c = 1.26$ GeV and gives in units of GeV:

$$4.79 \leqslant M_{Y_{cd}} \leqslant 5.73$$
$$\text{for } 5.02 \leqslant \sqrt{t_c} \leqslant 7 \text{ and } m_c = 1.26,$$
$$5.29 \leqslant M_{Y_{cd}} \leqslant 6.11$$
$$\text{for } 5.5 \leqslant \sqrt{t_c} \leqslant 7 \text{ and } m_c = 1.47. \tag{16}$$

We compare in Fig. 1(b), the t_c-behavior of the LSR results obtained at the τ-stability points with the ones from $\mathcal{R}_{cd}^{FESR}$ for the charm quark mass $m_c = 1.23$ GeV (running) and 1.47 GeV (on-shell). One can deduce the common solution in units of GeV:

$$M_{Y_{cd}} = 4.814 \quad \text{for } \sqrt{t_c} = 5.04(5) \text{ and } m_c = 1.26,$$
$$= 5.409 \quad \text{for } \sqrt{t_c} = 5.6 \text{ and } m_c = 1.47. \tag{17}$$

In order to fix the values of $M_{Y_{cd}}$ obtained at this lowest order PT calculations, we can also refer to the predictions of the J/ψ mass using the LSR at the same lowest order PT calculations and including the condensate contributions up to dimension six. We observe that the on-shell c-quark mass value tends to overestimate $M_{J/\psi}$ [2,27]. The same feature happens for the evaluation of the $X(1^{++})$ four-quark state mass [1]. Though this observation may not be rigorous as the strength of the radiative corrections is channel dependent, we are tempted to take as a final result in this Letter the prediction obtained by using the running mass $\overline{m}_c(m_c) = 1262(17)$ MeV within which it is known, from different examples in the literature, that the PT series converge faster [27].[7]

Including different sources of errors, we deduce in MeV[8]:

$$M_{Y_{cd}} = 4814(50)_{t_c}(14)_{m_c}(2)_{\Lambda}(17)_{\bar{u}u}(2)_{G^2}(4)_{M_0^2}(13)_{G^3}(6)_{\rho}$$
$$= 4814(57). \tag{18}$$

Using the fact that the 1st FESR moment gives a correlation between the mass of the lowest ground state and the onset of continuum threshold t_c, where its value coincide approximately with the value of the 1st radial excitation mass (see e.g. Ref. [39] and some other examples in [5]), we shall approximately identify its value with the one of the radial excitation. In order to take into account the systematics of the approach and some eventual small local duality violation advocated by [46] which can only be detectable in a high-precision analysis like the extraction of α_s from τ-decay [28,47], we have allowed t_c to move around this intersection point. Assuming that the mass of the radial excitation is approximately $\sqrt{t_c}$, one can deduce the mass-splitting:

$$M'_{Y_{cd}} - M_{Y_{cd}} \approx 226 \text{ MeV}, \tag{19}$$

which is similar to the one obtained for the $X(1^{++})$ four-quark state [1]. This splitting is much lower than the one intuitively used in the current literature:

$$M_\psi(2S) - M_\psi(1S) \simeq 590 \text{ MeV}, \tag{20}$$

for fixing the arbitrary value of t_c entering in different Borel (exponential) sum rules of the four-quark and molecule states. This dif-

---

[7] We plan to check this conjecture in a future publication when PT radiative corrections are included.

[8] We consider this result as an improvement (smaller error) of the one e.g. in [17] where only exponential sum rules have been used. However, the present error and the existing ones in the literature may have been underestimated due to the non-inclusion of the unknown PT radiative corrections and some eventual systematics of the approach.
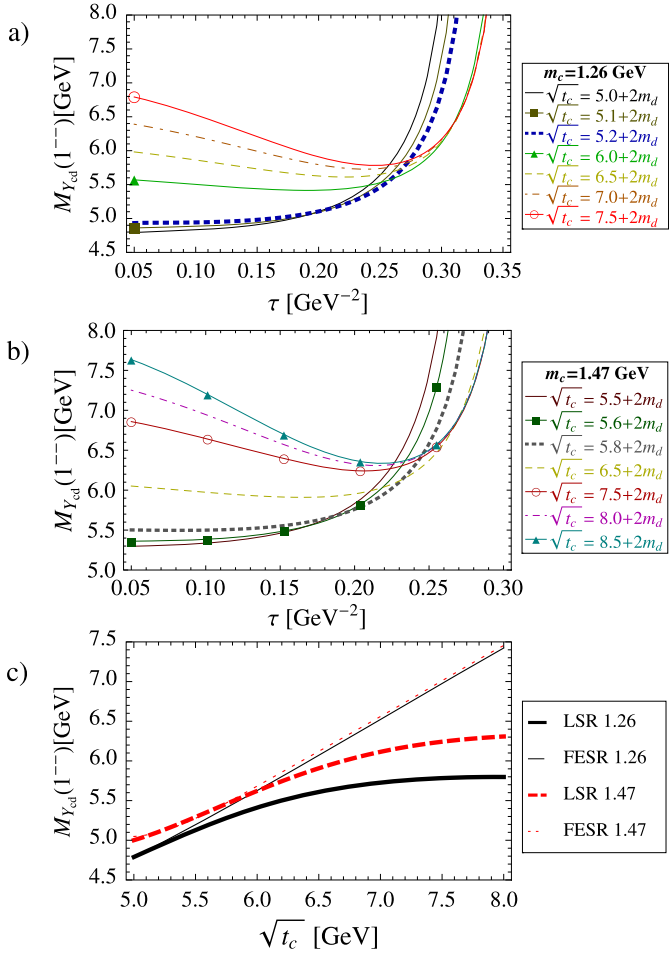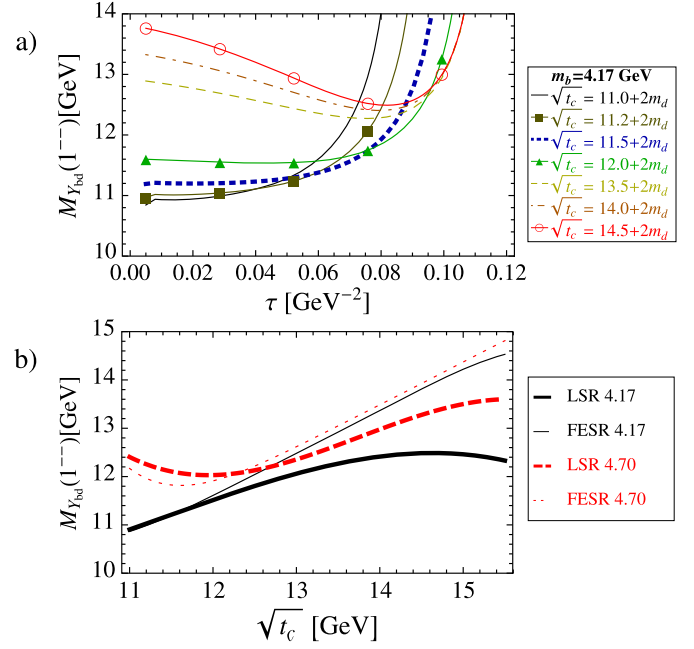
Fig. 1. (a) τ-behavior of $M_{Y_{cd}}(1^{--})$ from $\mathcal{R}^{LSR}_{cd}$ for the current mixing parameter $b = 0$, for different values of t_c and for $m_c = 1.26$ GeV; (b) the same as (a) but for $m_c = 1.47$ GeV; (c) t_c-behavior of the LSR results obtained at the τ-stability points and comparison with the ones from $\mathcal{R}^{FESR}_{cd}$ for $m_c = 1.26$ and 1.47 GeV.

ference may signal some new dynamics for the exotic states compared with the usual $\bar{c}c$ charmonium states and need to be tested from some other approaches such as potential models, heavy quark symmetry, AdS/QCD and lattice calculations.

3.2. The Y_{bd} mass from LSR and FESR for the case $b = 0$

Using similar analysis for the b-quark, we show the τ-behavior of $\mathcal{R}^{LSR}_{bd}(\tau)$ in Fig. 2(a) for $m_b = 4.17$ GeV and for different values of t_c. In Fig. 2(b), the same analysis is shown for $m_b = 4.70$ GeV. The most conservative result from the LSR is (in units of GeV) is:

$11.0 \leqslant M_{Y_{bd}} \leqslant 12.4$ for $11.2 \leqslant \sqrt{t_c} \leqslant 14.5$ and $m_b = 4.17$,

$12.1 \leqslant M_{Y_{bd}} \leqslant 13.4$ for $12.2 \leqslant \sqrt{t_c} \leqslant 15.5$ and $m_b = 4.70$,

where the lower (resp. higher) values of t_c correspond to the beginning of τ (resp. t_c)-stability. We compare in Fig. 2(b), the t_c-behavior of the LSR results obtained at the τ-stability points with the ones from $\mathcal{R}^{FESR}_{bd}$ for the b quark mass $m_b = 4.17$ GeV (running) and 4.70 GeV (on-shell). One can deduce the common solution in units of GeV:

$M_{Y_{bd}} = 11.26$ for $\sqrt{t_c} = 11.57(7)$ and $m_b = 4.17$,

$\quad = 12.09$ for $\sqrt{t_c} = 12.2$ and $m_b = 4.70$. (21)

Fig. 2. (a) τ-behavior of $M_{Y_{bd}}(1^{--})$ from $\mathcal{R}^{LSR}_{bd}$ for the current mixing parameter $b = 0$, for different values of t_c and for $m_b = 4.17$ GeV. (b) t_c-behavior of the LSR results obtained at the τ-stability points and comparison with the ones from $\mathcal{R}^{FESR}_{bd}$ for $m_b = 4.17$ and 4.70 GeV.

One can notice, like in the case of the charm quark that the value of the on-shell quark mass tends to give a higher value $M_{Y_{bd}}$ of within this lowest order PT calculations. Considering, like in the case of charm, as a final estimate the one from the running b-quark mass $\overline{m}_b(m_b) = 4177(11)$ MeV [27], we deduce in MeV:

$M_{Y_{bd}} = 11\,256(45)_{t_c}(8)_{m_b}(2)_\Lambda(15)_{\bar{u}u}(1)_{G^2}(1)_{M_0^2}(1)_{G^3}(5)_\rho$

$\quad = 11\,256(49).$ (22)

From the previous result, one can deduce the approximate value of the mass-splitting between the 1st radial excitation and the lowest mass ground state:

$M'_{Y_{bd}} - M_{Y_{bd}} \approx M'_{Y_{cd}} - M_{Y_{cd}} \approx 250\,\text{MeV},$ (23)

which are (almost) heavy-flavor independent and also smaller than the one of the bottomium splitting:

$M_\Upsilon(2S) - M_\Upsilon(1S) \simeq 560\,\text{MeV}.$ (24)

3.3. Effect of the current mixing b on the mass

In the following, we shall let the current mixing parameter b defined in Table 2 free and study its effect on the results obtained in Eqs. (18) and (22). In so doing, we fix the values of τ around the τ-stability point and t_c around the intersection point of the LSR and FESR. The results of the analysis are shown in Fig. 3. We notice that the results are optimal at the value $b = 0$ which a posteriori justifies the results obtained previously for $b = 0$.

3.4. Effect of the current mixing b on the decay constant $f_{Y_{Qd}}$

For completing the analysis of the effect of b, we also study the decay constant $f_{Y_{Qd}}$ defined as:

$\langle 0|j^\mu_{4q}|Y_{Qd}\rangle = f_{Y_{Qd}}M^4_{Y_{Qd}}\epsilon^\mu.$ (25)
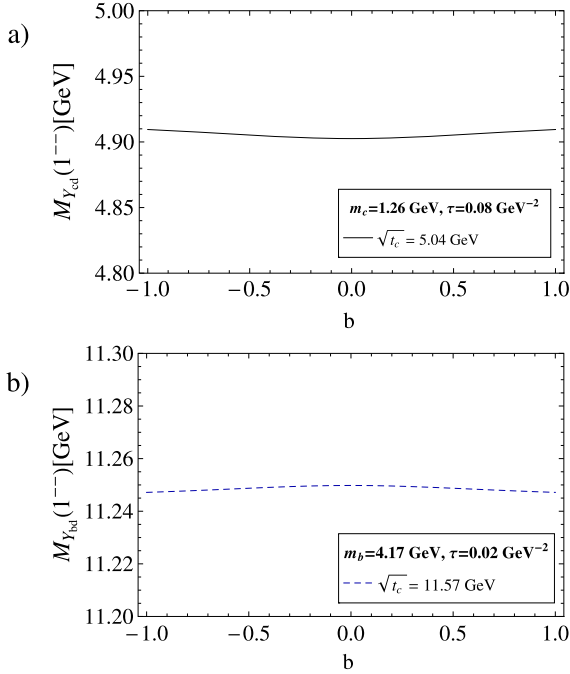
Fig. 3. (a) b-behavior of $M_{Y_{cd}}$ for given values of τ and t_c and for $m_c = 1.26$ GeV; (b) the same as (a) but for $M_{Y_{bd}}$ and for $m_b = 4.17$ GeV.

We show the analysis in Fig. 4 giving $M_{Y_{Qd}}$ and the corresponding t_c obtained above. One can deduce the optimal values at $b = 0$:

$$f_{Y_{cd}} \simeq 0.08 \text{ MeV} \quad \text{and} \quad f_{Y_{bd}} \simeq 0.03 \text{ MeV}, \tag{26}$$

which are much smaller than $f_\pi = 132$ MeV, $f_\rho \simeq 215$ MeV and $f_D \simeq f_B = 203$ MeV [48]. On can also note that the decay constant decreases like $1/M_Q$ which can be tested in HQET or/and lattice QCD.

3.5. SU(3) breaking for $M_{Y_{Qs}}$ from DRSR

We study the ratio $M_{Y_{Qs}}/M_{Y_{Qd}}$ using double ratio of LSR (DRSR):

$$r_{sd}^Q \equiv \frac{\sqrt{\mathcal{R}_{Qs}^{LSR}}}{\sqrt{\mathcal{R}_{Qd}^{LSR}}} \quad \text{where } Q \equiv c, b. \tag{27}$$

We show the τ-behavior of r_{sd}^c and r_{sd}^b respectively in Fig. 5(a), (b) for $m_c = 1.26$ GeV and $m_b = 4.17$ GeV for different values of t_c. We show, in Fig. 5(c), (d), the t_c-behavior of the stabilities or inflexion points for two different values (running and on-shell) of the quark masses. One can see in these figures that the DRSR is very stable versus the t_c variations in the case of the running heavy quark masses. We deduce the corresponding DRSR:

$$r_{sd}^c = 1.018(1)_{m_c}(5)_{m_s}(2)_\kappa(2)_{\bar{u}u}(1)_\rho,$$
$$r_{sd}^b = 1.007(0.5)_{m_b}(2)_{m_s}(0.5)_\kappa(1)_{\bar{u}u}(0.3)_\rho, \tag{28}$$

respectively for $\sqrt{t_c} = 5.1$ and 11.6 GeV. Using the results for Y_{Qd} in Eqs. (18) and (22) and the values of the $SU(3)$ breaking ratio in Eq. (28), we can deduce the mass of the Y_{Qs} state in MeV:

$$M_{Y_{cs}} = 4900(67), \qquad M_{Y_{bs}} = 11\,334(55), \tag{29}$$

leading to the $SU(3)$ mass-splitting:

$$\Delta M_{sd}^{Y_c} \approx 87 \text{ MeV} \approx \Delta M_{sd}^{Y_b} \approx 78 \text{ MeV}, \tag{30}$$
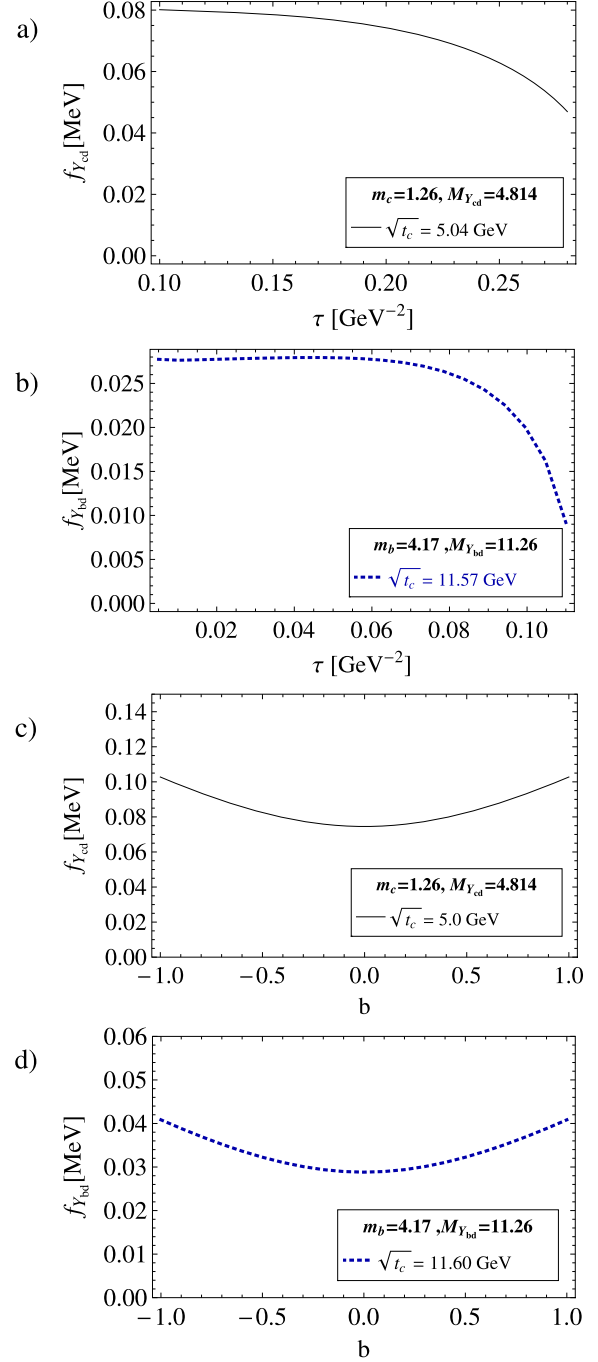
which is also (almost) heavy-flavor independent.

Fig. 4. (a) τ-behavior of $f_{Y_{cd}}$ for given values of $b = 0$ and t_c and for $m_c = 1.26$ GeV; (b) the same as (a) but for $f_{Y_{bd}}$ and for $m_b = 4.17$ GeV; (c) b-behavior of $f_{Y_{cd}}$ for given values of τ at the stability and t_c; (d) the same as (c) but for $f_{Y_{bd}}$.

4. 1^{--} molecule masses from QSSR

4.1. The $\bar{D}^*_{d(s)} D_{d(s)}$ and $\bar{B}^*_{d(s)} B_{d(s)}$ molecules[9]

Like in the previous case, we use LSR and FESR for studying the masses of the $\bar{D}^*_d D_d$ and $\bar{B}^*_d B_d$ and DRSR for studying the $SU(3)$ breaking ratios:

---

[9] Hereafter, for simplifying notations, D and B denote the scalar D_0^* and B_0^* mesons.

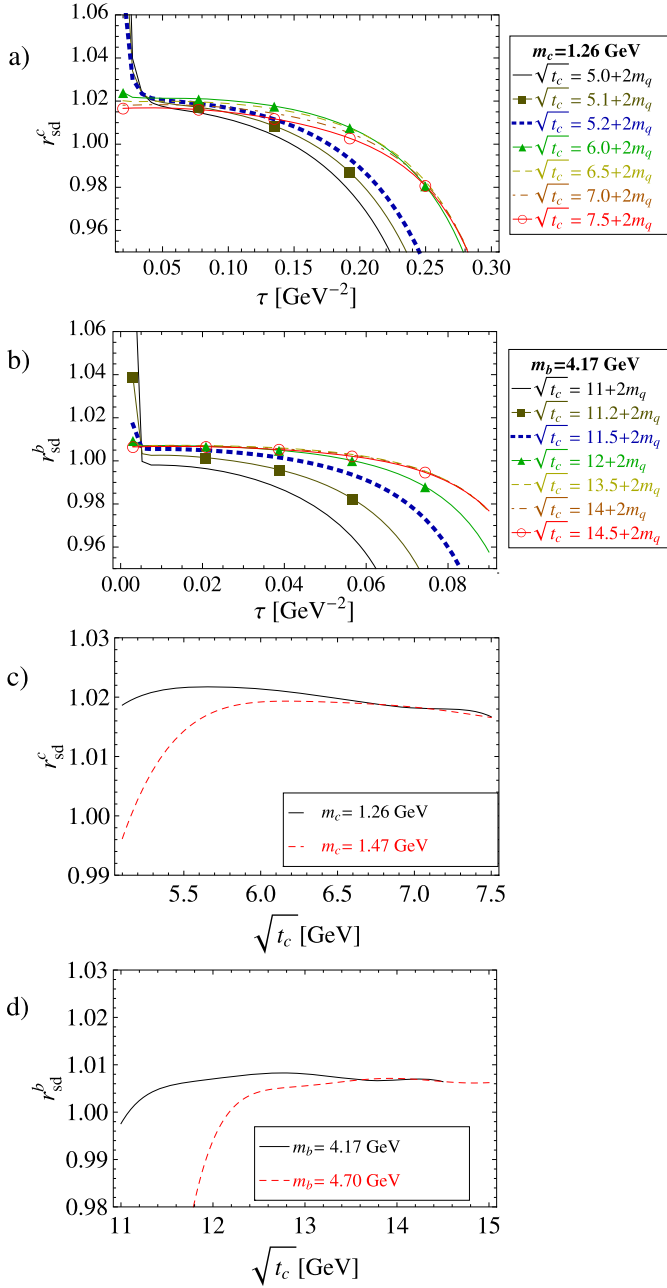**Fig. 5.** (a) τ-behavior of r_{sd}^c for the current mixing parameter $b = 0$, for different values of t_c and for $m_c = 1.26$ GeV; (b) τ-behavior of r_{sd}^b for different values of t_c and for $m_b = 4.17$ GeV; (c) t_c-behavior of the inflexion points (or minimas) of r_{sd}^c from (a); (d) the same for the b quark using r_{sd}^b from (b).

$$r_{sd}^D \equiv \frac{M_{D_s^* D_s}}{M_{D_d^* D_d}}, \qquad r_{sd}^B \equiv \frac{M_{B_s^* B_s}}{M_{B_d^* B_d}}. \tag{31}$$

We show their τ-behavior for different values of t_c and for $m_c = 1.26$ GeV and $m_b = 4.17$ GeV respectively in Figs. 6(a), (b) and 7(a), (b). The t_c-behavior of the τ-minimas is shown in Fig. 6(c), (d) for the masses and in Fig. 7(c), (d) for the $SU(3)$ breaking ratios. Using the sets ($m_c = 1.26$ GeV, $\sqrt{t_c} = 5.58$ GeV) and ($m_b = 4.17$ GeV, $\sqrt{t_c} = 11.64(3)$ GeV) common solutions of LSR and FESR, one can deduce in MeV:

$$M_{D_d^* D_d} = 5268(14)_{m_c}(3)_\Lambda(19)_{\bar{u}u}(0)_{G^2}(0)_{M_0^2}(2)_{G^3}(5)_\rho,$$
$$= 5268(24),$$

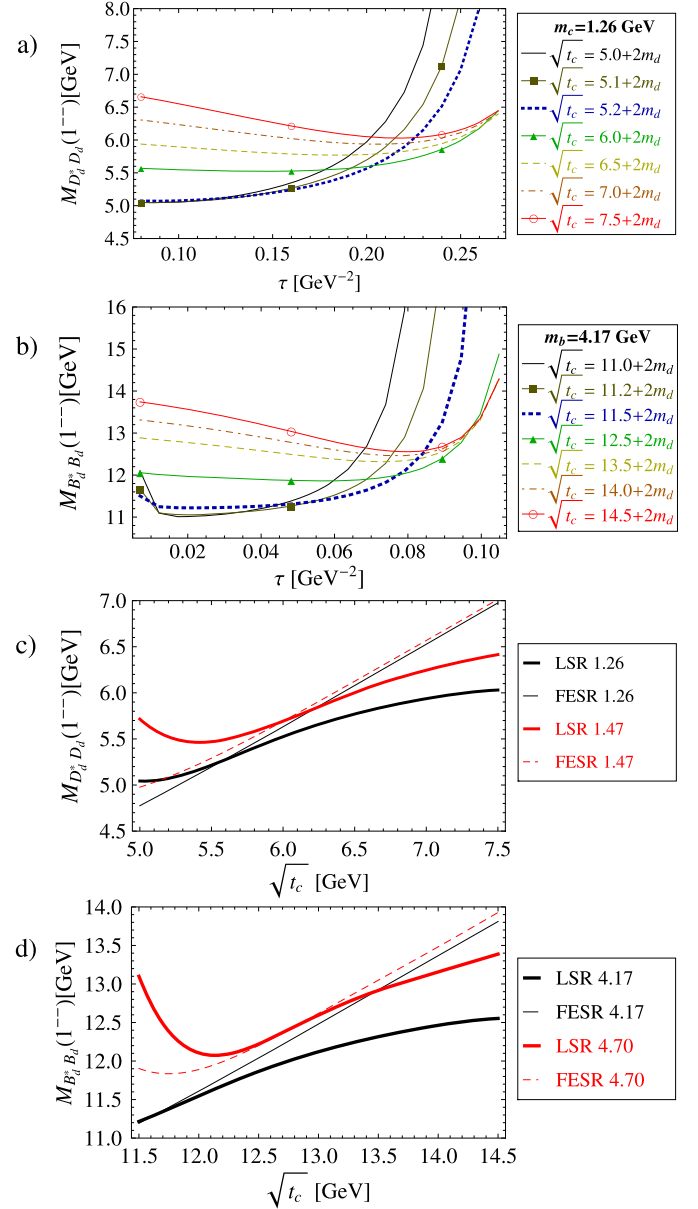**Fig. 6.** (a) τ-behavior of $M_{D_d^* D_d}$ for different values of t_c and for $m_c = 1.26$ GeV; (b) τ-behavior of $M_{B_d^* B_d}$ for different values of t_c and for $m_b = 4.17$ GeV; (c) t_c-behavior of the extremas in τ of $M_{D_d^* D_d}$ and for $m_c = 1.26$–1.47 GeV; (d) the same as (c) but for $M_{B_d^* B_d}$ and for $m_b = 4.17$–4.70 GeV.

$$M_{B_d^* B_d} = 11\,302(20)_{t_c}(9)_{m_b}(2)_\Lambda(19)_{\bar{u}u}(0)_{G^2}(0)_{M_0^2}(1)_{G^3}(5)_\rho$$
$$= 11\,302(30),$$

$$r_{sd}^D = 1.018(1)_{m_c}(4)_{m_s}(0.8)_\kappa(0.5)_{\bar{u}u}(0.2)_\rho(0.1)_{G^3},$$
$$r_{sd}^B = 1.006(1)_{m_b}(2)_{m_s}(1)_\kappa(0.5)_{\bar{u}u}(0.2)_\rho(0.1)_{G^3}. \tag{32}$$

Using the previous results in Eq. (32), one obtains in MeV:

$$M_{D_s^* D_s} = 5363(33), \qquad M_{B_s^* B_s} = 11\,370(40), \tag{33}$$

corresponding to a $SU(3)$ mass-splitting:

$$\Delta M_{sd}^{DD^*} \simeq 95 \text{ MeV} \approx \Delta M_{sd}^{BB^*} \simeq 68 \text{ MeV}. \tag{34}$$

These results for M_{DD^*} are in the upper part of the range given in [17] due both to the smaller values of $m_c = 1.23$ GeV and
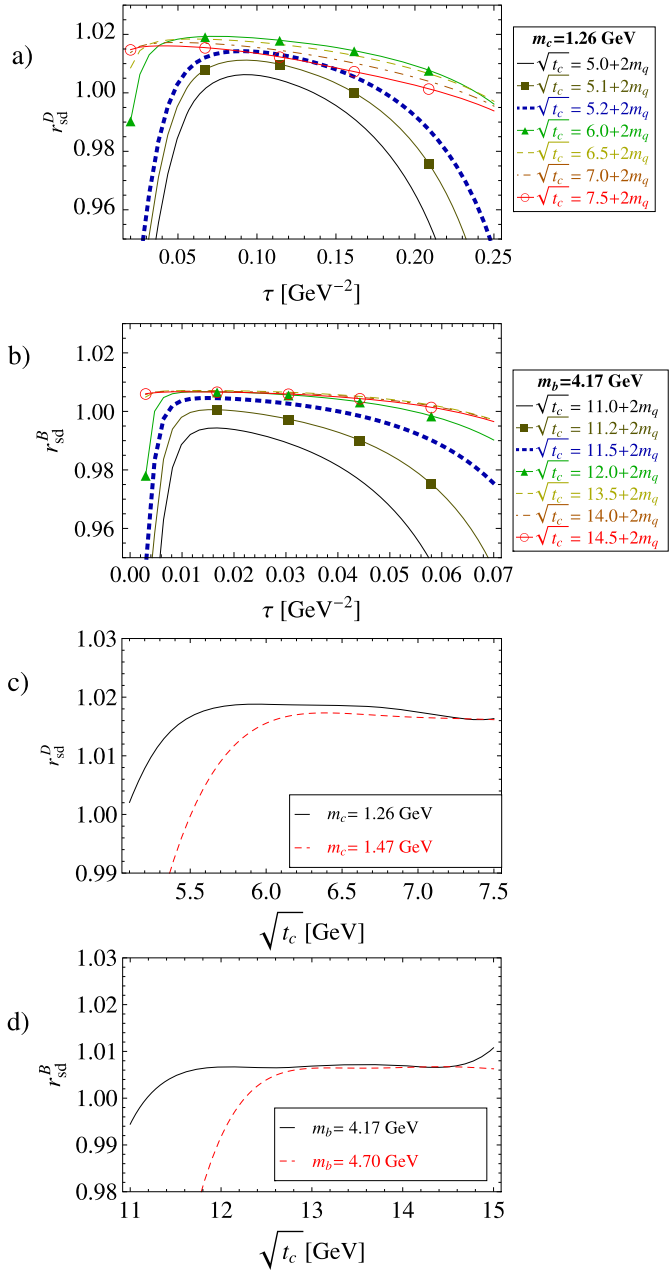
Fig. 7. (a) τ-behavior of r_{sd}^D for different values of t_c and for $m_c = 1.26$ GeV; (b) τ-behavior of r_{sd}^B for different values of t_c and for $m_b = 4.17$ GeV; (c) t_c-behavior of the inflexion points (or minimas) of r_{sd}^D from (a); (d) the same for the b quark using r_{sd}^B from (b).

$\sqrt{t_c} = 5.5$ GeV used in that paper. Though the DD^* molecule mass is above the DD^* threshold which is similar to the e.g. the case of the $\pi\pi$ continuum and ρ-meson resonance in e^+e^- to the $I = 1$ hadrons channel, one expects that at the τ-stability point or inside the sum rule window, where the QCD continuum contribution is minimum while the OPE is still convergent, the lowest ground state dominates the sum rule.

4.2. The $J/\psi S_2$ and ΥS_2 molecules

Combining LSR and FESR, we consider the mass of the $J/\psi S_2$ and ΥS_2 molecules in a color singlet combination, where $S_2 \equiv$
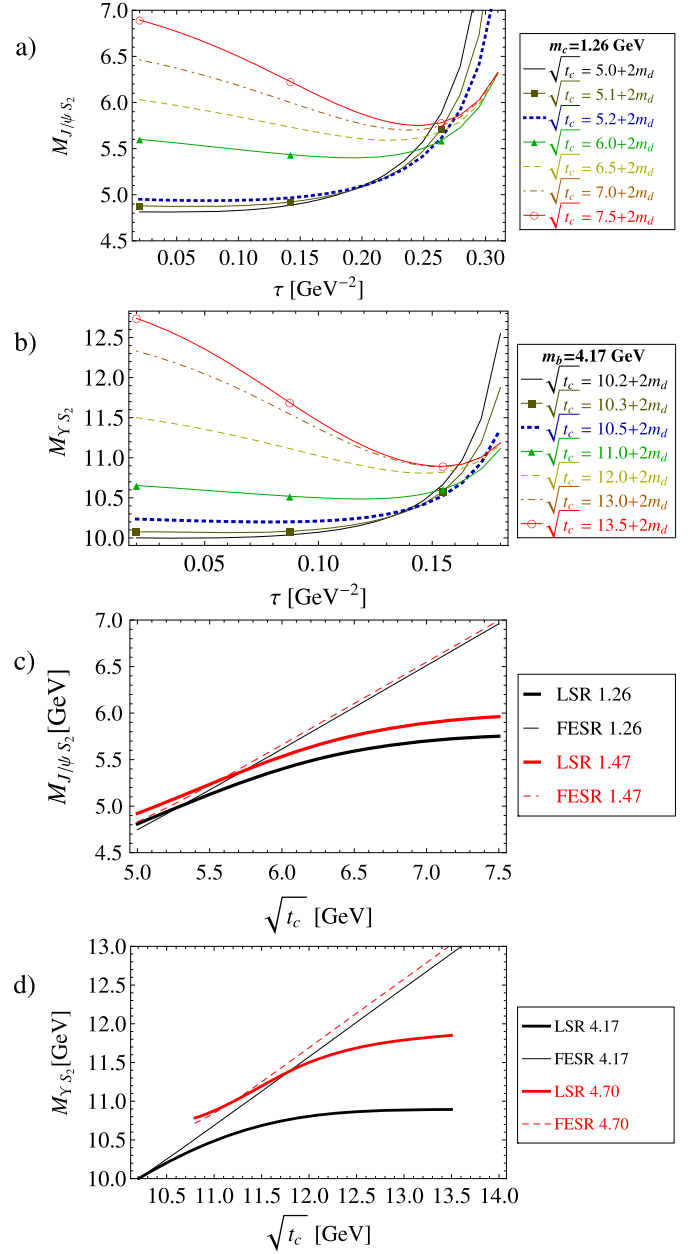

Fig. 8. (a) τ-behavior of $M_{J/\psi S_2}$ for different values of t_c and for $m_c = 1.26$ GeV; (b) τ-behavior of $M_{\Upsilon S_2}$ for different values of t_c and for $m_b = 4.17$ GeV; (c) t_c-behavior of the extremas in τ of $M_{J/\psi S_2}$ for $m_c = 1.26$–1.47 GeV; (d) the same as (c) but for $M_{\Upsilon S_2}$ for $m_b = 4.17$–4.70 GeV.

$\bar{u}u + \bar{d}d$ is a scalar meson.[10] In so doing, we work with the LO QCD expression obtained in [17]. We show the results versus the LSR variable τ in Fig. 8(a), (b). The t_c-behavior of different τ-extremas is given in Fig. 8(c), (d) from which we can deduce for the running quark masses for $\sqrt{t_c} = 5.30(2)$ and 10.23(3) GeV in units of MeV:

$$M_{J/\psi S_2} = 5002(20)_{t_c}(8)_{m_c}(2)_{\Lambda}(19)_{\bar{u}u}(9)_{G^2}(0)_{M_0^2}(0)_{G^3}(6)_{\rho}$$

$$= 5002(31),$$

---

[10] The low-mass $\pi^+\pi^-$ invariant mass due to the σ meson is expected to result mainly from its gluon rather than from its quark component [49,50] such that an eventual quark–gluon hybrid meson nature of the Y_c is also possible.
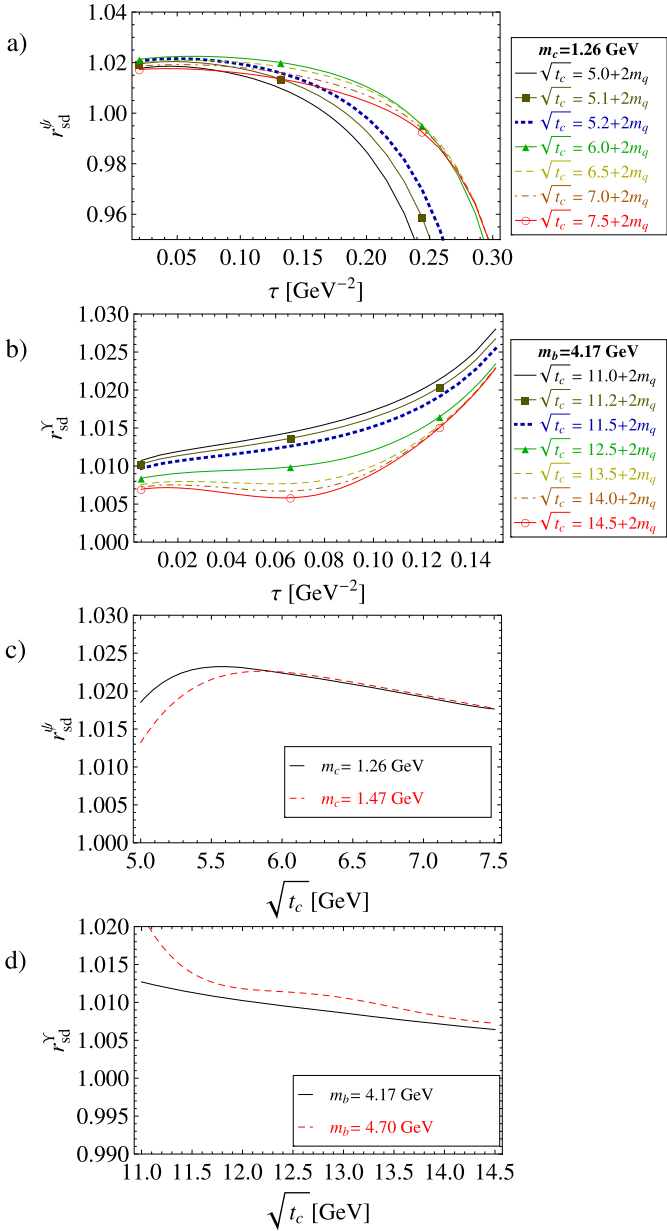
Fig. 9. (a) τ-behavior of r_{sd}^ψ for different values of t_c and for $m_c = 1.26$ GeV; (b) τ-behavior of r_{sd}^Υ for different values of t_c and for $m_b = 4.17$ GeV; (c) t_c-behavior of the extremas in τ of r_{sd}^ψ for $m_c = 1.26$–1.47 GeV; (d) the same as (c) but for r_{sd}^Υ for $m_b = 4.17$–4.70 GeV.

$$M_{\Upsilon S_2} = 10\,015(20)_{t_c}(9)_{m_b}(2)_\Lambda(16)_{\bar u u}(17)_{G^2}(0)_{M_0^2}(0)_{G^3}(5)_\rho$$
$$= 10\,015(33). \tag{35}$$

The splitting (in units of MeV) with the first radial excitation approximately given by $\sqrt{t_c}$ is:

$$M'_{J/\psi S_2} - M_{J/\psi S_2} \approx 298, \qquad M'_{\Upsilon S_2} - M_{\Upsilon S_2} \approx 213. \tag{36}$$

In the same way, we show in Fig. 9 the τ and t_c behaviors of the $SU(3)$ breaking ratios, from which, we can deduce:

$$r_{sd}^\psi \equiv \frac{M_{J/\psi S_3}}{M_{J/\psi S_2}} = 1.022(0.2)_{m_c}(5)_{m_s}(2)_\kappa,$$

$$r_{sd}^\Upsilon \equiv \frac{M_{\Upsilon S_3}}{M_{\Upsilon S_2}} = 1.011(1)_{m_b}(2)_{m_s}(0.2)_\kappa, \tag{37}$$

Table 4
Masses of the four-quark and molecule states from the present analysis combining Laplace (LSR) and finite energy (FESR). We have used double ratios (DRSR) of sum rules for extracting the $SU(3)$ mass-splittings. The results correspond to the value of the running heavy quark masses but the $SU(3)$ mass-splittings are less affected by such definitions. As already mentioned in the text for simplifying notations, D and B denote the scalar D_0^* and B_0^* mesons. The errors do not take into account the unknown ones from PT corrections.

States		States	
Four-quarks	1^{--}		0^{++}
Y_{cd}	4818(27)	Y_{cd}^0	6125(51)
Y_{cs}	4900(67)	Y_{cs}^0	6192(59)
Y_{bd}	11 256(49)	Y_{bd}^0	12 542(43)
Y_{bs}	11 334(55)	Y_{bs}^0	12 592(50)
Molecules	1^{--}		0^{++}
$\bar D_d^* D_d$	5268(24)	$\bar D_d D_d$	5955(48)
$\bar D_s^* D_s$	5363(33)	$\bar D_s D_s$	6044(56)
$\bar B_d^* B_d$	11 302(30)	$\bar B_d B_d$	11 750(40)
$\bar B_s^* B_s$	11 370(40)	$\bar B_s B_s$	11 844(50)
Singlet current	1^{--}	Octet current	1^{--}
$J/\psi S_2$	5002(31)		5118(29)
$J/\psi S_3$	5112(41)		5231(40)
ΥS_2	10 015(33)		10 268(28)
ΥS_3	10 125(40)		10 371(45)

where $S_3 \equiv \bar s s$ is a scalar meson. Then, we obtain in MeV:

$$M_{J/\psi S_3} = 5112(41), \qquad M_{\Upsilon S_3} = 10\,125(40), \tag{38}$$

corresponding to the $SU(3)$ mass-splittings:

$$\Delta M_{sd}^{J/\psi} \simeq \Delta M_{sd}^\Upsilon \approx 110 \text{ MeV}. \tag{39}$$

The mass-splittings in Eq. (39) are comparable with the ones obtained previously.

Doing the same exercise for the octet current, we deduce the results in Table 4 where the molecule associated to the octet current is 100 (resp. 250) MeV above the one of the singlet current for J/ψ (resp. Υ) contrary to the 1^{++} case discussed in [2]. The ratio of $SU(3)$ breakings are respectively 1.022(5) and 1.010(2) in the c and b channels which are comparable with the ones in Eq. (37). When comparing our results with the ones in Ref. [17], we notice that the low central value of $M_{J/\psi S_2}$ obtained there (which we reproduce) corresponds to a smaller value of $m_c = 1.23$ GeV and mainly to a low value of $\sqrt{t_c} = 5.1$ GeV which does not coincide with the common solution $\sqrt{t_c} = 5.3$ GeV from LSR and FESR. On the opposite, the large value of $M_{\Upsilon S_2} = 10.74$ (resp. 11.09) GeV obtained there corresponds to a too high value $\sqrt{t_c} = 11.3$ (resp. 11.7) GeV compared with the LSR and FESR solution $\sqrt{t_c} = 10.23$ (resp. 10.48) GeV for the singlet (resp. octet) current.

5. 0^{++} four-quark and molecule masses from QSSR

In the following, we extend the previous analysis to the case of the 0^{++} mesons.

5.1. Y_{Qd}^0 mass and decay constant from LSR and FESR

We do the analysis of the Y_{cd}^0 and Y_{bd}^0 masses using LSR and FESR. We show the results in Fig. 10 for the current mixing parameter $b = 0$ from which we deduce in MeV, for the running quark masses, and respectively for $\sqrt{t_c} = 6.5$ and 13.0 GeV where LSR and FESR match:

$$M_{Y_{cd}^0} = 6125(16)_{m_c}(7)_\Lambda(44)_{\bar u u}(12)_{G^2}(14)_\rho$$
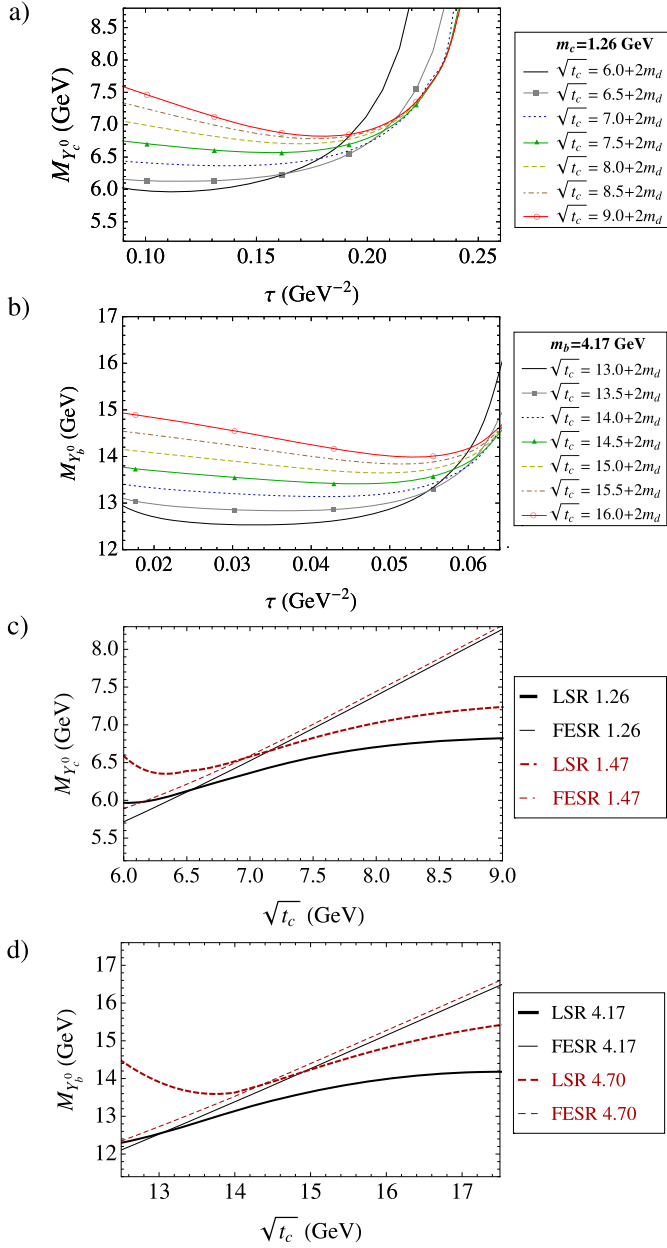$$= 6125(51) \text{ MeV},$$

Fig. 10. (a) τ-behavior of Y_{cd}^0 for the current mixing parameter $b = 0$, for different values of t_c and for $m_c = 1.26$ GeV; (b) τ-behavior of Y_{bd}^0 for different values of t_c and for $m_b = 4.17$ GeV; (c) t_c-behavior of the extremas in τ of Y_{cd}^0 for $m_c = 1.26$–1.47 GeV; (d) the same as (c) but for Y_{bd}^0 for $m_b = 4.17$–4.70 GeV.

$$M_{Y_{bd}^0} = 12\,542(22)_{t_c}(13)_{m_b}(1)_\Lambda(7)_{\bar{u}u}(34)_{G^2}(2)_\rho$$
$$= 12\,542(43) \text{ MeV.} \tag{40}$$

One can notice that the splittings between the lowest ground state and the 1st radial excitation approximately given by $\sqrt{t_c}$ is in MeV:

$$M_{Y_{cd}^0}' - M_{Y_{cd}^0} \approx 375, \qquad M_{Y_{bd}^0}' - M_{Y_{bd}^0} \simeq 464, \tag{41}$$

which is larger than the ones of the 1^{--} states, comparable with the ones of the J/ψ and Υ, and are (almost) heavy-flavor independent. We show in Fig. 11 the effect of the choice of b operator mixing parameter on the mass predictions, indicating an optimal value at $b = 0$. For completeness, we show in Fig. 12 the τ and b behaviors of the decay constants from which we deduce:
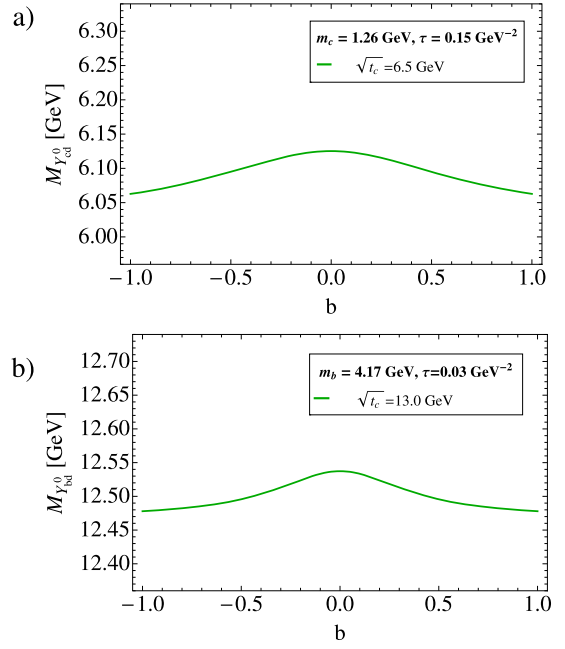

Fig. 11. (a) b-behavior of $M_{Y_{cd}^0}$ for given values of τ and t_c and for $m_c = 1.26$ GeV; (b) the same as (a) but for $M_{Y_{bd}^0}$ and for $m_b = 4.17$ GeV.

$$f_{Y_{cd}^0} \simeq 0.12 \text{ MeV} \quad \text{and} \quad f_{Y_{bd}^0} \simeq 0.03 \text{ MeV}, \tag{42}$$

which are comparable with the ones of the spin 1 case in Eq. (26).

5.2. SU(3) breaking for $M_{Y_{Qs}}^0$ from DRSR

We show in Figs. 13 the τ and t_c behaviors of the SU(3) breaking ratios for the current mixing parameter $b = 0$:

$$r_{sd}^{0Q} \equiv \frac{Y_{Qs}^0}{Y_{Qd}^0}: \quad Q \equiv c, b, \tag{43}$$

from which we deduce:

$$r_{sd}^{0c} = 1.011(2)_{m_c}(3.8)_{m_s}(1.4)_\kappa(1)_{\bar{u}u}(0.7)_\rho,$$
$$r_{sd}^{0b} = 1.004(1)_{m_c}(1.7)_{m_s}(0.3)_\kappa, \tag{44}$$

leading (in units of MeV) to:

$$M_{Y_{cs}^0} = 6192(59), \qquad M_{Y_{bs}^0} = 12\,592(50), \tag{45}$$

and the SU(3) mass-splittings:

$$\Delta M_{sd}^{Y_c^0} \simeq 67 \approx \Delta M_{sd}^{Y_b^0} \simeq 50 \text{ MeV.} \tag{46}$$

5.3. $M_{D_d D_d}$ and $M_{B_d B_d}$ from LSR and FESR

We show the τ and t_c behaviors of the masses $M_{D_d D_d}$ and $M_{B_d B_d}$ in Fig. 14. Like in previous sections, we consider as a final result (in units of MeV) the one corresponding to the running masses for $\sqrt{t_c} = 6.25(3)$ and 12.02 GeV:

$$M_{D_d D_d} = 5955(24)_{t_c}(14)_{m_c}(5)_\Lambda(36)_{\bar{u}u}(4)_{G^2}(4)_{G^3}(12)_\rho$$
$$= 5955(48),$$

$$M_{B_d B_d} = 11\,750(12)_{m_b}(4)_\Lambda(35)_{\bar{u}u}(7)_{G^2}(3)_{G^3}(12)_\rho$$
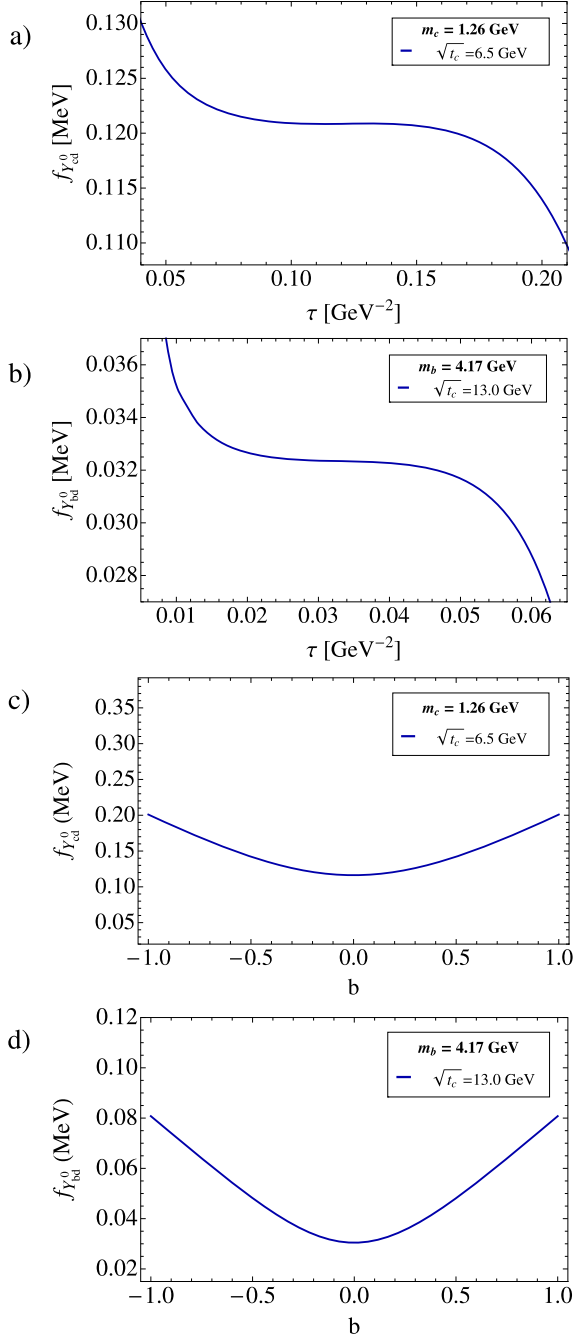$$= 11\,750(40). \tag{47}$$

Fig. 12. (a) τ-behavior of $f_{Y^0_{cd}}$ for given values of $b = 0$ and t_c and for $m_c = 1.26$ GeV; (b) the same as (a) but for $f_{Y^0_{bd}}$ and for $m_b = 4.17$ GeV; (c) b-behavior of $f_{Y^0_{cd}}$ at the τ-stability and for a given value of t_c; (d) the same as (c) but for $f_{Y^0_{bd}}$.

One can notice that the splittings between the lowest ground state and the 1st radial excitation approximately given by $\sqrt{t_c}$ is in MeV:

$$M'_{D_d D_d} - M_{D_d D_d} \approx 290, \qquad M'_{B_d B_d} - M_{B_d B_d} \approx 270, \qquad (48)$$

which, like in the case of the 1^{--} states are smaller than the ones of the J/ψ and Υ, and almost heavy-flavor independent.

5.4. SU(3) breaking for $M_{\bar{D}_s D_s}$ and $M_{\bar{B}_s B_s}$ from DRSR

We show in Fig. 15 the τ-behavior of the $SU(3)$ mass ratios for different values of t_c and the t_c behavior of their τ-extremas. Therefore, we deduce:
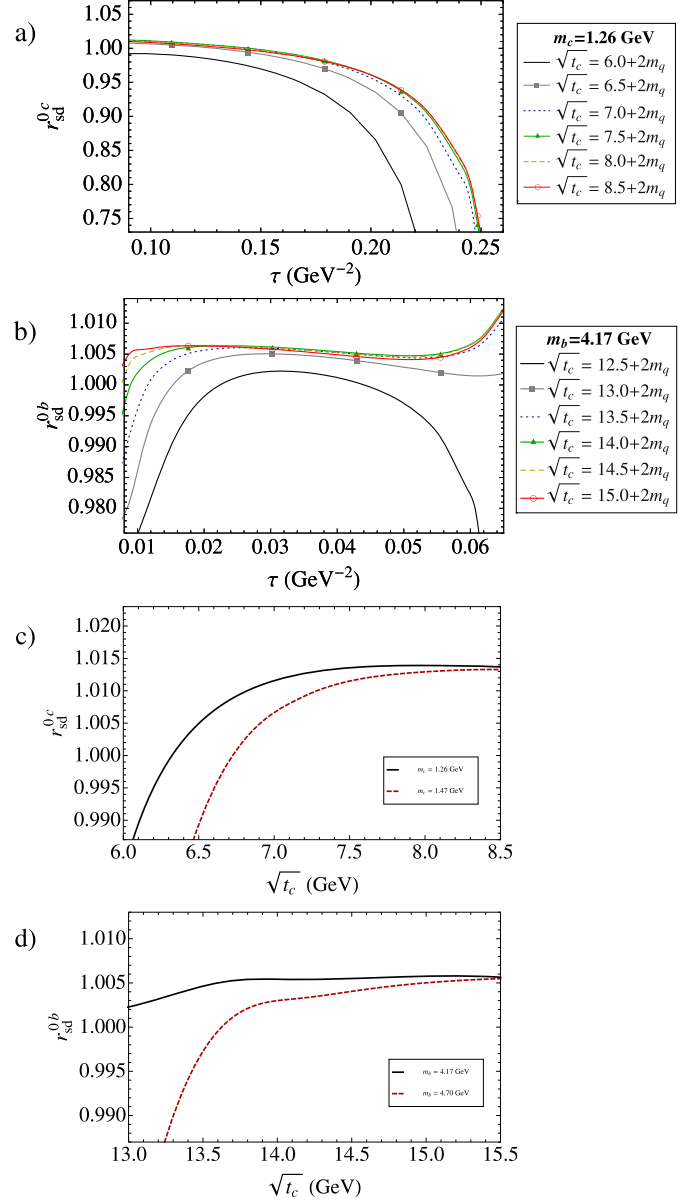

Fig. 13. (a) τ-behavior of r^{0c}_{sd} for the current mixing parameter $b = 0$, for different values of t_c and for $m_c = 1.26$ GeV; (b) τ-behavior of r^{0b}_{sd} for different values of t_c and for $m_b = 4.17$ GeV; (c) t_c-behavior of the extremas in τ of r^{0c}_{sd} for $m_c = 1.26$–1.47 GeV; (d) the same as (c) but for r^{0b}_{sd} for $m_b = 4.17$–4.70 GeV.

$$r^{0D}_{sd} \equiv \frac{M_{D_s D_s}}{M_{D_d D_d}} = 1.015(1)_{m_c}(4)_{m_s}(2)_\kappa(1)_{\bar{u}u}(0.5)_\rho,$$

$$r^{0B}_{sd} \equiv \frac{M_{B_s B_s}}{M_{B_d B_d}} = 1.008(1)_{m_c}(4)_{m_s}(2)_\kappa(1)_{\bar{u}u}(0.5)_\rho. \qquad (49)$$

Using the previous values of $M_{D_d D_d}$ and $M_{B_d B_d}$, we deduce in MeV:

$$M_{D_s D_s} = 6044(56), \qquad M_{B_s B_s} = 11\,844(50), \qquad (50)$$

which corresponds to a $SU(3)$ splitting:

$$\Delta M^{DD}_{sd} \approx 89 \text{ MeV} \approx \Delta M^{BB}_{sd} \approx 94 \text{ MeV}. \qquad (51)$$

6. Summary and conclusions

We have studied the spectra of the 1^{--} and 0^{++} four-quarks and molecules states by combining Laplace (LSR) and finite energy
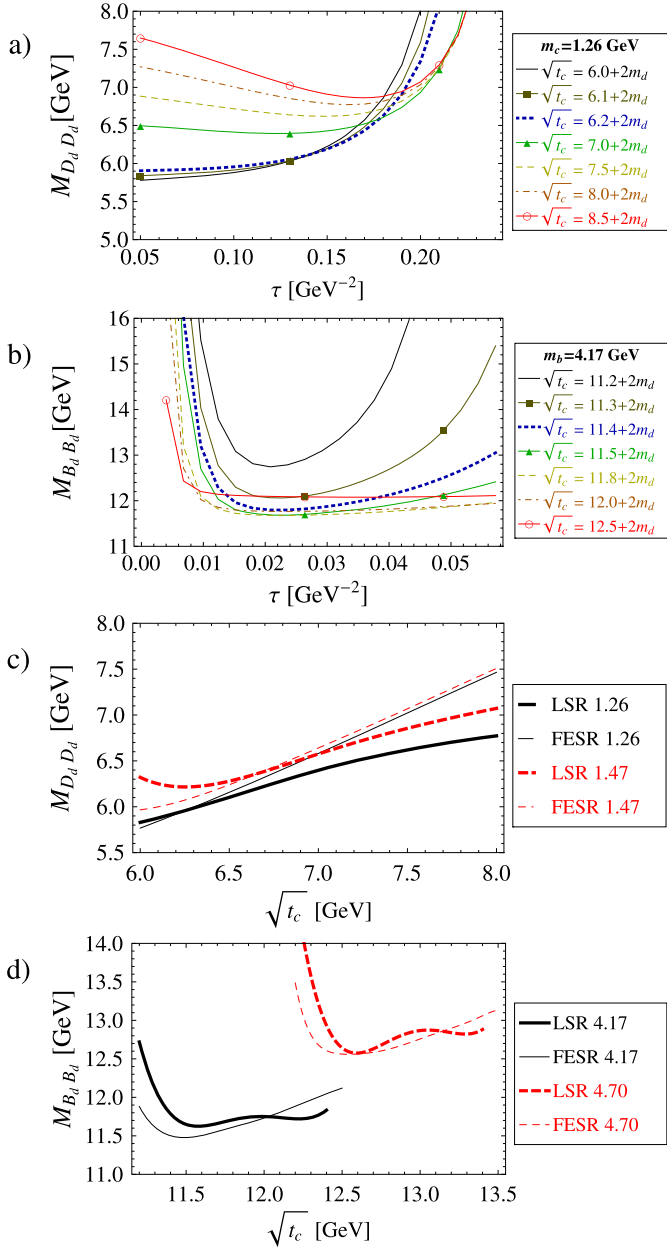
Fig. 14. (a) τ-behavior of $M_{D_d D_d}$ for different values of t_c and for $m_c = 1.26$ GeV; (b) τ-behavior of $M_{B_d B_d}$ for different values of t_c and for $m_b = 4.17$ GeV; (c) t_c-behavior of the extremas in τ of $M_{D_d D_d}$ and for $m_c = 1.26$–1.47 GeV; (d) the same as (c) but for $M_{B_d B_d}$ and for $m_b = 4.17$–4.70 GeV.
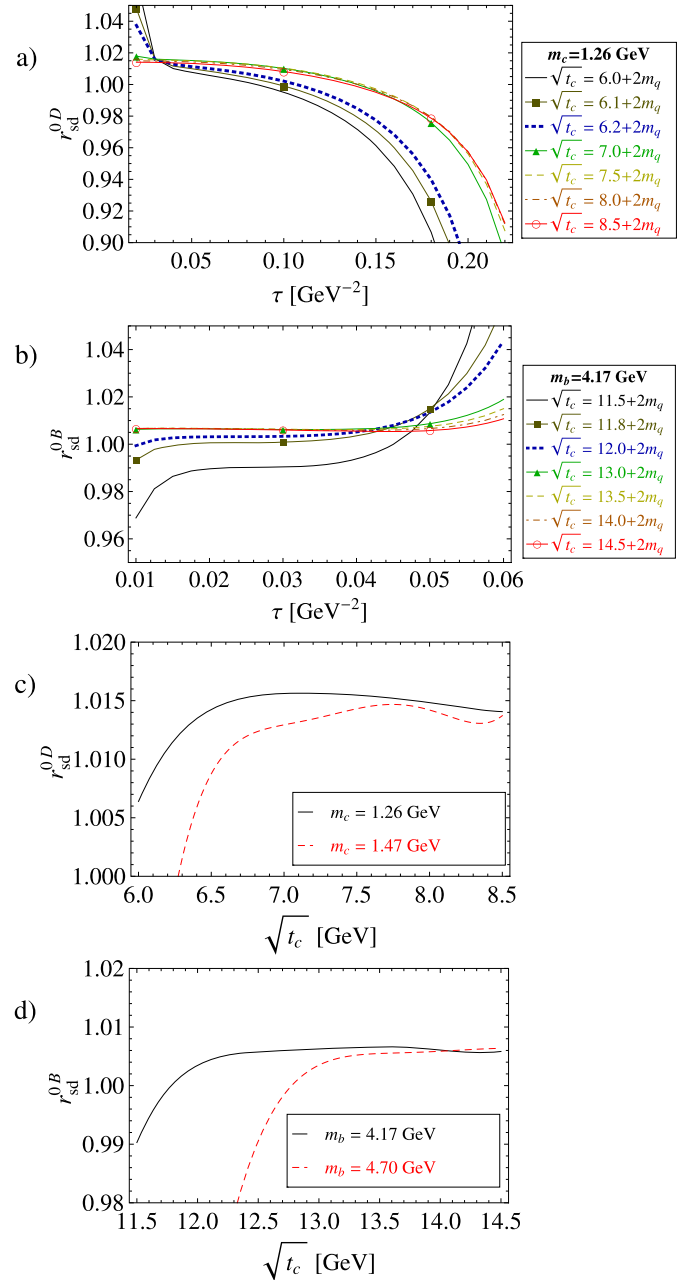
Fig. 15. (a) τ-behavior of r_{sd}^D for different values of t_c and for $m_c = 1.26$ GeV; (b) τ-behavior of r_{sd}^B for different values of t_c and for $m_b = 4.17$ GeV; (c) t_c-behavior of the inflexion points (or minimas) of r_{sd}^D from Fig. 7(a); (d) the same for the b quark using r_{sd}^B from Fig. 7(b).

(FESR) sum rules. The $SU(3)$ mass-splittings have been obtained using double ratios of sum rules (DRSR). We consider the present results as improvement of the existing ones in the literature extracted only from LSR where the criterion for fixing the value of the continuum thresholds are often ad hoc or based on the ones of the standard charmonium/bottomium systems mass-splittings which are not confirmed by the present analysis. Our results are summarized in Table 4. We find that:

- The three $Y_c(4260, 4360, 4660)$ 1^{--} experimental candidates are too low for being pure four-quark or/and molecule $\bar{D}D^*$ and $J/\psi S_2$ states but can result from their mixings. The $Y_b(10890)$ is lower than the predicted values of the four-quark and $\bar{B}B^*$ molecule masses but heavier than the predicted ΥS_2 and ΥS_3 molecule states. Our results may indi-

cate that some other natures (hybrids, threshold effects, ...) of these states are not excluded. On can notice that our predictions for the masses are above the corresponding meson–meson thresholds indicating that these exotic states can be weakly bounded.

- For the 1^{--}, there is a regularity of about (250–300) MeV for the value of the mass-splittings between the lowest ground state and the 1st radial excitation roughly approximated by the value of the continuum threshold $\sqrt{t_c}$ at which the LSR and FESR match. These mass-splittings are (almost) flavor-independent and are much smaller than the ones of 500 MeV of ordinary charmonium and bottomium states and do not support some ad hoc choice used in the literature for

fixing the t_c-values when extracting the optimal results from the LSR.

- There is also a regularity of about 50–90 MeV for the $SU(3)$ mass-splittings of the different states which are also (almost) flavor-independent.
- The spin 0 states are much more heavier ($\geqslant 400$ MeV) than the spin 1 states, like in the case of hybrid states [5].
- The decay constants of the 1^{--} and 0^{++} four-quark states obtained in Eqs. (26) and (42) are much smaller than f_π, f_ρ and $f_{D,B}$. Unlike f_B expected to behave as $1/\sqrt{M_Q}$, the four-quark states decay constants exhibit a $1/M_Q$ behavior which can be tested using HQET or/and lattice QCD.

It is likely that some other non-perturbative approaches such as potential models, HQET, AdS/QCD and lattice calculations check the previous new features and values on mass-splittings, mass and decay constants derived in this Letter. We also expect that present and future experiments (LHCb, Belle, BaBar, ...) can test our predictions.

Acknowledgements

References

[1] R.D. Matheus, S. Narison, M. Nielsen, J.M. Richard, Phys. Rev. D 75 (2007) 014005;
J.M. Dias, S. Narison, F.S. Navarra, M. Nielsen, J.M. Richard, Phys. Lett. B 703 (2011) 274.
[2] S. Narison, F.S. Navarra, M. Nielsen, Phys. Rev. D 83 (2011) 016004.
[3] For reviews, see e.g. E.S. Swanson, Phys. Rept. 429 (2006) 243;
J.M. Richard, Nucl. Phys. B (Proc. Suppl.) 164 (2007) 131;
F.S. Navarra, M. Nielsen, S.H. Lee, Phys. Rep. 497 (2010) 41;
N. Brambilla, et al., Eur. Phys. J. C 71 (2011) 1534;
S.L. Zhu, Int. J. Mod. Phys. E 17 (2008) 283.
[4] M.A. Shifman, A.I. Vainshtein, V.I. Zakharov, Nucl. Phys. B 147 (1979) 385;
M.A. Shifman, A.I. Vainshtein, V.I. Zakharov, Nucl. Phys. B 147 (1979) 448.
[5] For reviews, see e.g. S. Narison, QCD as a Theory of Hadrons, Cambridge Monographs on Particle Physics, Nuclear Physics and Cosmology, vol. 17, Cambridge Univ. Press, Cambridge, 2002, arXiv:hep-ph/0205006;
S. Narison, QCD Spectral Sum Rules, World Scientific Lecture Notes in Physics, vol. 26, World Scientific, Singapore, 1989;
S. Narison, Acta Phys. Pol. B 26 (1995) 687;
S. Narison, Phys. Rept. 84 (1982) 263;
S. Narison, arXiv:hep-ph/9510270, 1995.
[6] L.J. Reinders, H. Rubinstein, S. Yazaki, Phys. Rept. 127 (1985) 1.
[7] S. Narison, Phys. Lett. B 210 (1988) 238.
[8] S. Narison, Phys. Lett. B 387 (1996) 162;
S. Narison, Phys. Lett. B 605 (2005) 319;
S. Narison, Phys. Lett. B 322 (1994) 327;
S. Narison, Phys. Rev. D 74 (2006) 034013;
S. Narison, Phys. Lett. B 358 (1995) 113;
S. Narison, Phys. Lett. B 466 (1999) 34.
[9] R.M. Albuquerque, S. Narison, Phys. Lett. B 694 (2010) 217;
R.M. Albuquerque, S. Narison, M. Nielsen, Phys. Lett. B 684 (2010) 236.
[10] S. Narison, Phys. Lett. B 337 (1994) 166;
S. Narison, Phys. Lett. B 668 (2008) 308.
[11] S.-K. Choi, et al., Belle Collaboration, Phys. Rev. Lett. 91 (2003) 262001.
[12] B. Aubert, et al., BaBar Collaboration, Phys. Rev. D 71 (2005) 071103.
[13] D. Acosta, et al., CDF II Collaboration, Phys. Rev. Lett. 93 (2004) 072001.
[14] V.M. Abazov, et al., D0 Collaboration, Phys. Rev. Lett. 93 (2004) 162002.
[15] W. Chen, S.L. Zhu, Phys. Rev. D 83 (2011) 034010.
[16] A. Bondar, et al., Belle Collaboration, Phys. Rev. Lett. 108 (2012) 122001;
I. Adachi, et al., Belle Collaboration, arXiv:1207.4345, 2012;
R. Mussa, Belle Collaboration, talk given at QCD 12, Montpellier, 2–6 July 2012.
[17] R.M. Albuquerque, M. Nielsen, Nucl. Phys. A 815 (2009) 53;

[18] Q. He, et al., CLEO Collaboration, Phys. Rev. D 74 (2006) 091104;
T.E. Coan, et al., CLEO Collaboration, Phys. Rev. Lett. 96 (2006) 162003.
[19] B. Aubert, et al., BaBar Collaboration, arXiv:0808.1543v2 [hep-ex];
B. Aubert, et al., BaBar Collaboration, Phys. Rev. D 98 (2007) 212001.
[20] X.L. Wang, et al., Belle Collaboration, Phys. Rev. Lett. 99 (2007) 142002;
C.Z. Yuan, et al., Belle Collaboration, Phys. Rev. Lett. 99 (2007) 182004.
[21] T. Aaltonen, et al., CDF Collaboration, arXiv:1101.6058v1 [hep-ex], 2011.
[22] K.-F. Chen, et al., Belle Collaboration, Phys. Rev. D 82 (2010) 091106R.
[23] E. Bagan, M. Chabab, H.G. Dosch, S. Narison, Phys. Lett. B 301 (1993) 243;
A. Khodjamirian, Ch. Klein, Th. Mannel, Y.-M. Wang, JHEP 1109 (2011) 106.
[24] E.G. Floratos, S. Narison, E. de Rafael, Nucl. Phys. B 155 (1979) 155.
[25] S. Narison, R. Tarrach, Phys. Lett. B 125 (1983) 217.
[26] M. Jamin, M. Kremer, Nucl. Phys. B 277 (1986) 349;
V. Spiridonov, K.G. Chetyrkin, Sov. J. Nucl. Phys. 47 (1988) 522.
[27] S. Narison, Phys. Lett. B 693 (2010) 559;
S. Narison, Phys. Lett. B 705 (2011) 544 (Erratum);
S. Narison, Phys. Lett. B 706 (2011) 412;
S. Narison, Phys. Lett. B 707 (2012) 259.
[28] S. Narison, Phys. Lett. B 673 (2009) 30.
[29] E. Braaten, S. Narison, A. Pich, Nucl. Phys. B 373 (1992) 581;
S. Narison, A. Pich, Phys. Lett. B 211 (1988) 183.
[30] For reviews, see e.g. S. Narison, Phys. Rev. D 74 (2006) 034013;
S. Narison, arXiv:hep-ph/0202200;
S. Narison, Nucl. Phys. B (Proc. Suppl.) 86 (2000) 242;
S. Narison, Phys. Lett. B 216 (1989) 191;
S. Narison, Phys. Lett. B 358 (1995) 113;
S. Narison, Phys. Lett. B 466 (1999) 345;
S. Narison, Riv. Nuovo Cimento 10 (2) (1987) 1;
S. Narison, H.G. Dosch, Phys. Lett. B 417 (1998) 173;
S. Narison, N. Paver, E. de Rafael, D. Treleani, Nucl. Phys. B 212 (1983) 365;
S. Narison, E. de Rafael, Phys. Lett. B 103 (1981) 57;
C. Becchi, S. Narison, E. de Rafael, F.J. Yndurain, Z. Phys. C 8 (1981) 335.
[31] K. Nakamura, et al., Particle Data Group, J. Phys. G 37 (2010) 075021.
[32] S. Narison, Phys. Lett. B 197 (1987) 405;
S. Narison, Phys. Lett. B 341 (1994) 73;
S. Narison, Phys. Lett. B 520 (2001) 115.
[33] B.L. Ioffe, K.N. Zyablyuk, Eur. Phys. J. C 27 (2003) 229;
B.L. Ioffe, Prog. Part. Nucl. Phys. 56 (2006) 232.
[34] Y. Chung, et al., Z. Phys. C 25 (1984) 151;
H.G. Dosch, in: S. Narison (Ed.), Conference of Non-Perturbative Methods, Montpellier, 1985, World Scientific, Singapore, 1985;
H.G. Dosch, M. Jamin, S. Narison, Phys. Lett. B 220 (1989) 251.
[35] B.L. Ioffe, Nucl. Phys. B 188 (1981) 317;
B.L. Ioffe, Nucl. Phys. B 191 (1981) 591;
A.A. Ovchinnikov, A.A. Pivovarov, Yad. Fiz. 48 (1988) 1135.
[36] S. Narison, Phys. Lett. B 605 (2005) 319.
[37] G. Launer, S. Narison, R. Tarrach, Z. Phys. C 26 (1984) 433.
[38] S. Narison, Phys. Lett. B 300 (1993) 293;
S. Narison, Phys. Lett. B 361 (1995) 121.
[39] R.A. Bertlmann, G. Launer, E. de Rafael, Nucl. Phys. B 250 (1985) 61;
R.A. Bertlmann, et al., Z. Phys. C 39 (1988) 231.
[40] F.J. Yndurain, arXiv:hep-ph/9903457.
[41] S. Narison, Phys. Lett. B 387 (1996) 162.
[42] J.S. Bell, R.A. Bertlmann, Nucl. Phys. B 227 (1983) 435;
R.A. Bertlmann, Acta Phys. Austriaca 53 (1981) 305;
R.A. Bertlmann, H. Neufeld, Z. Phys. C 27 (1985) 437.
[43] S. Narison, Phys. Lett. B 361 (1995) 121;
S. Narison, Phys. Lett. B 624 (2005) 223;
S. Narison, Phys. Lett. B 520 (2001) 115.
[44] K. Chetyrkin, S. Narison, V.I. Zakharov, Nucl. Phys. B 550 (1999) 353;
S. Narison, V.I. Zakharov, Phys. Lett. B 522 (2001) 266;
S. Narison, V.I. Zakharov, Phys. Lett. B 679 (2009) 355.
[45] For reviews, see e.g. V.I. Zakharov, Nucl. Phys. B (Proc. Suppl.) 164 (2007) 240;
S. Narison, Nucl. Phys. B (Proc. Suppl.) 164 (2007) 225.
[46] M.A. Shifman, arXiv:hep-ph/0009131.
[47] O. Catà, M. Golterman, S. Peris, Phys. Rev. D 77 (2008) 0930064.
[48] S. Narison, Phys. Lett. B 198 (1987) 104.
[49] S. Narison, G. Veneziano, Int. J. Mod. Phys. A 4 (1989) 2751;
S. Narison, Nucl. Phys. B 509 (1998) 312.
[50] P. Minkowski, W. Ochs, Eur. Phys. J. C 9 (1999) 283;
G. Mennessier, S. Narison, W. Ochs, Phys. Lett. B 665 (2008) 205;
G. Mennessier, S. Narison, W. Ochs, Nucl. Phys. B (Proc. Suppl.) 238 (2008) 181;
G. Mennessier, P. Minkowski, S. Narison, W. Ochs, in: HEPMAD 07 Conference, SLAC Econf C0709107, 2007, arXiv:0707.4511 [hep-ph];
R. Kaminski, G. Mennessier, S. Narison, Phys. Lett. B 680 (2009) 148;
G. Mennessier, S. Narison, X.-G. Wang, Phys. Lett. B 688 (2010) 59;
G. Mennessier, S. Narison, X.-G. Wang, Phys. Lett. B 696 (2011) 40.